AXIOM YOUNG RESEARCH

Original Research Articles in

International Journal of Student Mathematics & Science

Volume 2

Mathematics
Applied Science
Computational Thinking-
Scientific Modeling

A Platform for the Next Generation of Scientists

Axiom Journal

INTERNATIONAL JOURNAL

AXIOM YOUNG RESEARCH

International Journal of Student Mathematics and Science

VOLUME 2

CONTRIBUTORS

Jinu Yoon

Aisha Shermatova

Hayeon Ku

Raina Chae

Matthew Su, Kaian Solomon, Jimmy Thompson, James Cunningham

Yong Jin Chang

WWW.AXIOMJOURNAL.ORG

EMAIL
admin@axiomjournal.org

ADDRESS
Dept. of Mathematics New Academic Block, University of Delhi, New Delhi 110007 India

MATHEMATICS · APPLIED SCIENCE

SCIENTIFIC MODELING

A PLATFORM FOR THE NEXT GENERATION OF SCIENTISTS

Where curiosity becomes discovery.

EXPLORING IDEAS. ADVANCING YOUNG SCIENCE.

> *Axiom Young Research is an international journal dedicated to publishing original research conducted by young scholars in mathematics, science, and interdisciplinary STEM fields. The journal provides a professional platform where students can present rigorous ideas, develop scientific thinking, and share their discoveries with the global academic community. By encouraging curiosity, logical reasoning, and independent inquiry, Axiom Young Research seeks to inspire the next generation of scientists and mathematicians.*

Editorial Note

VOLUME 2 EDITION

The advancement of science and mathematics depends on curiosity, creativity, and rigorous thinking. These qualities are not limited by age. Many important discoveries in the history of science began with simple questions asked by young minds.

Axiom Young Research was established to provide a professional platform where young scholars can present original ideas and develop their research abilities through the process of academic writing and publication.

This journal encourages students to move beyond routine problem solving and to engage in deeper exploration of mathematical structures, scientific phenomena, and computational ideas. Through independent research, students learn how to formulate questions, construct logical arguments, analyze data, and communicate results clearly.

The articles presented in this volume reflect the intellectual curiosity and dedication of students from diverse backgrounds who share a passion for discovery. Each contribution represents not only a research result but also a step in the development of future scientists and scholars.

We hope that this journal will inspire more students to pursue independent inquiry and contribute to the global scientific community.

A PLATFORM FOR THE NEXT GENERATION OF SCIENTISTS

JOURNAL FOUNDATION

Introduction

Scientific discovery often begins with a simple question.

> *Why does this pattern occur?*
>
> *Is there a hidden structure behind this phenomenon?*
>
> *Can mathematics explain what we observe in the world?*

Many of the most important ideas in science and mathematics started with curiosity and careful observation. Axiom Young Research was created to support young scholars who are eager to explore such questions and to transform their ideas into structured research.

The journal encourages students to move beyond traditional classroom learning and engage in independent investigation. By developing hypotheses, constructing mathematical arguments, building models, and analyzing data, students gain experience in the authentic practice of scientific inquiry.

Axiom Young Research provides a platform where these ideas can be shared with a broader academic community.

CORE PRINCIPLES

Our Philosophy

The philosophy of Axiom Young Research is founded on several core principles.

CURIOSITY DRIVES DISCOVERY

Scientific and mathematical exploration begins with curiosity. When students ask deeper questions and seek logical explanations, they begin the journey toward genuine research.

IDEAS HAVE NO AGE LIMIT

Important insights can emerge at any stage of learning. Young researchers often bring fresh perspectives and creative approaches to problems that have been studied for generations.

RIGOR MATTERS

Even at the student level, research should be guided by clear reasoning, careful analysis, and intellectual honesty. Axiom Young Research encourages students to develop these habits early in their academic journey.

ACCESS TO RESEARCH SHOULD BE OPEN

Opportunities for scholarly publication should not be limited by financial barriers or institutional privilege. The journal strives to make academic participation accessible to students from diverse backgrounds around the world.

THE FUTURE OF SCIENCE BEGINS WITH STUDENTS

Today's young researchers will become tomorrow's scientists, mathematicians, engineers, and innovators. By providing a platform for early academic exploration, Axiom Young Research supports the development of the next generation of thinkers and problem solvers.

MESSAGE FROM THE BOARD

Head Director's Message

The beginning of every meaningful discovery lies in a question.

Young students often possess an extraordinary curiosity about the world. They observe patterns, challenge assumptions, and attempt to explain complex ideas using the tools of mathematics and science. Unfortunately, many of these ideas remain confined to classrooms or personal notebooks, never reaching a wider audience.

Axiom Young Research was established to change that.

Our goal is to provide talented students with the opportunity to experience the process of academic research and publication. Writing a research paper requires more than simply presenting results; it demands careful reasoning, clear communication, and intellectual discipline. Through this process, students learn how to develop ideas, evaluate evidence, and present arguments in a scholarly manner.

We believe that intellectual curiosity should be encouraged at every stage of education. By supporting young researchers and providing them with a professional platform to share their work, Axiom Young Research hopes to inspire a lifelong engagement with mathematics, science, and discovery.

We are honored to present the work of young scholars who represent the future of scientific and mathematical inquiry.

HEAD DIRECTOR

Hemant Kumar Singh

Contents

Axiom Journal

Modeling Food Spoilage Using Exponential Bacterial Growth

Jinu Yoon

USA, The Webb Schools, GRADE: 9

Modeling Food Spoilage Using Exponential Bacterial Growth

Jinu Yoon
USA, The Webb Schools , GRADE: 9

Abstract

This study investigates how temperature affects food spoilage through a mathematical model based on exponential bacterial growth. Starting from the observation that food lasts significantly longer in a refrigerator than at room temperature, we explore the underlying cause: the rapid multiplication of microorganisms. By modeling bacterial growth with exponential functions, we compare the spoilage process under different storage conditions. Using sashimi as a case study, we calculate the respective growth rates for refrigerated and room-temperature environments. Our results show that sashimi, which remains safe for 72 hours in a refrigerator, can become unsafe in just 2 hours at room temperature. Furthermore, we demonstrate how even brief exposure to warm conditions such as 10 minutes outside the fridge can reduce remaining shelf life by as much as 6 hours. This model not only explains the importance of proper food storage but also provides a quantitative tool for understanding food safety guidelines.

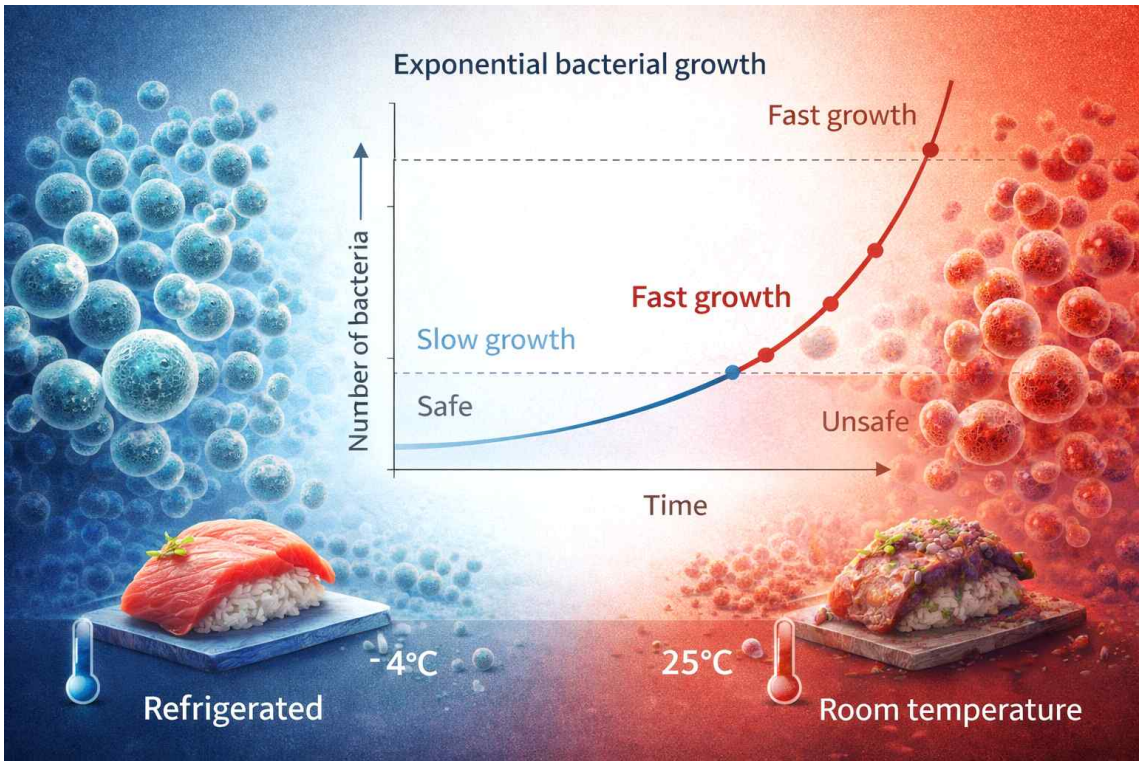

1. Introduction

Food spoils easily because of microorganisms like bacteria and fungi. Though these organisms are too small to see, they reproduce quickly and cause food to go bad. To slow down this process, people often use refrigerators, which can keep food fresh much longer than leaving it at room temperature.

This research began with a simple question: Why does food last for several days in a refrigerator but spoil within just a few hours at room temperature? For example, milk can stay fresh for about two weeks in the fridge, yet may turn sour in less than six hours if left out. Clearly, this difference can't be explained by time alone. We realized that the rate at which microorganisms grow must be the key, and we decided to explore this idea using mathematics.

In this paper, we use exponential functions to build a mathematical model of how food spoils over time. We assume that the number of microorganisms increases exponentially, meaning their population grows faster and faster. This model helps us understand how storage conditions affect food safety and allows us to estimate when food becomes unsafe to eat.

Chapter 2 explains why exponential growth is a reasonable assumption, using simple examples to show how quickly microorganisms can multiply. Chapter 3 compares their growth in cold and warm environments and calculates the changes when food is moved between them. Chapter 4 applies this model to real-life situations and explores how it helps us interpret food safety guidelines. Finally, Chapter 5 summarizes our findings and reflects on what we've learned about spoilage and storage through this mathematical approach.

2. Understanding exponential models

To understand why food spoils, we first need to know how microorganisms grow. These tiny organisms reproduce by making copies of themselves, and this can happen very quickly. For example, one bacterium might turn into three. In the next hour, each of those three makes two more, turning into nine. As you can see, the number of bacteria increases very fast.

Let's look at a simple case. Suppose we begin with just one bacterium, and every hour it makes two more. That means:

- After 1 hour → 3 bacteria
- After 2 hours → 9 bacteria
- After 3 hours → 27 bacteria
- After 4 hours → 81 bacteria

This pattern follows the rule:

$$\text{Number of bacteria after } t \text{ hours} = 3^t$$

This is called exponential growth. It's different from linear growth, where the number increases by the same amount each hour. With exponential growth, the numbers get much bigger, much faster.

If the environment is warmer or more suitable, bacteria can grow even more quickly. For example, if one bacterium creates four new ones each hour, it becomes five in total after one hour. Then the number of bacteria grows like this:

$$\text{Number of bacteria after } t \text{ hours} = 5^t$$

This increases much faster than 3^t. The number at the base of the exponent (in this case, 3 or 5) depends on how favorable the environment is. That's why food spoils faster in warm places.

In general, if we start with P bacteria and the growth is exponential, the number of bacteria after ttt hours is:

$$P \times x^t$$

Here, $x > 1$ is the growth rate, which changes based on the environment, and t is time. In cold places like refrigerators, x is smaller. In warm places like room temperature, t is larger.

In the next chapter, we'll use this formula to compare how bacteria grow in different environments, and how this affects food safety.

3. Main Body

When sashimi is freshly produced after being caught, it contains a small number of bacteria. Let us call the number of bacteria at this stage P.

We assume that if the number of bacteria goes over $10000P$, the sashimi is no longer safe to eat. In other words, $10000P$ is the benchmark for spoilage. This number is not chosen randomly for convenience, but a standard which was proven by public health regulations.

Due to safety rules, we should try to keep the number of bacteria in fresh food below the $\frac{1}{10000}$ of the spoilage threshold. That is why the initial amount is kept at or below P. Food must be stored or handled in a way that keeps the number of bacteria within this safe range.

We summarize these ideas with the following assumptions:

Assumption 1. The initial number of bacteria is P

Assumption 2. The food is considered spoiled when the number of bacteria exceeds $10000P$.

Let us now define the growth factor in a refrigerator as x and the growth factor at room temperature as y. Since bacteria grows faster at higher temperature, we have the inequality $1 < x < y$.

We can now express the number of bacteria after t hours of storage using the variables of the previous chapter. If the food is kept in a refrigerator, the number of bacteria becomes:

$$P \times x^t$$

If kept at room temperature, the number becomes:

$$P \times y^t.$$

Clearly, the shelf life of food depends on the method of its storage. As mentioned in the introduction, sashimi can stay safe for about 3 days in a fridge but may become unsafe after only 2 hours at room temperature.

In the case of refrigeration, we can find the shelf life by solving the equation:

$$P \times x^t = 10000P$$

We cancel A from both sides and take the logarithm with base x:

$$t = \log_x 10000$$

Using the change-of-base formula for logarithms, we get:

$$t = \frac{\log 10000}{\log x}.$$

Here, the log means the common logarithm with base 10. In the same way, for food stores at room temperature, we solve:

$$P \times y^t = 10000P$$

This gives:

$$t = \frac{\log 10000}{\log y}.$$

Since $1 < x < y$, it follows that $0 < \log x < \log y$. Therefore, the shelf life at room temperature is shorter than the shelf life in a refrigerator.

In the next chapter, we will apply this model to sashimi.

4. Applying the Model to Sashimi

Let us now apply our model to sashimi. Suppose that sashimi can be kept safely in a refrigerator for about 3 days. This is equal to:

$$3 \text{ days } = 72 \text{ hours.}$$

From Chapter 3, we know that the shelf in a refrigerator is given by

$$72 = \frac{4}{\log x}$$

and it yields

$$x = 10^{\frac{1}{18}} \approx 1.1364$$

Now let us consider room temperature. Suppose that sashimi becomes unsafe after 2 hours outside the fridge. Then we use:

$$2 = \frac{4}{\log y}$$

and it yields

$$y = 10^2 = 100$$

Let us now use this model to understand what happens when sashimi is taken out of the refrigerator and not returned right away. Suppose the sashimi is freshly produced and taken out of the refrigerator, but it is left at room temperature for 10 minutes. This is a realistic situation. Since 10 minutes is one third of an hour, we set $t = \frac{1}{6}$. The number of bacteria after 10 minutes becomes:

$$P \times y^{\frac{1}{6}} = P \times 10^{\frac{1}{3}}$$

Now suppose the milk is immediately placed back into the refrigerator. From that point, bacteria grow according to the refrigeration rate x. So, after t more hours in the fridge, the number of bacteria becomes:

$$P \times 10^{\frac{1}{3}} \times x^t$$

We find the remaining shelf life by solving:

$$P \times 10^{\frac{1}{3}} \times x^t = 10000P$$

It is equivalent to $x^t = \frac{10000}{10^{\frac{1}{3}}} = 10^{4-\frac{1}{3}} = 10^{\frac{11}{3}}$.

Now, take log to both sides to get

$$t\log x = \frac{11}{3}.$$

From $x = 10^{\frac{1}{18}}$, we have $\log x = \frac{1}{18}$ and we can conclude that

$$t = \frac{11}{3} \times 18 = 66$$

So the remaining shelf life is 66 hours, Originally, the shelf life was 72 hours. Just 10 minutes outside the fridge has diminished the shelf life by:

$$72 - 66 = 6 \text{ hours.}$$

This shows how even a short time at room temperature can greatly reduce how long sashimi stays safe.

5. Conclusion

In this paper, we used exponential functions to model how food spoils over time due to the increase of the number of bacteria. We assumed that freshly produced food contains a small number of bacteria, and that the food becomes spoiled when the number of bacteria grows to 10000 times the original amount.

We also assumed that the growth rate of bacteria depends on the environment like temperature. Specifically, bacteria grow much faster at room temperature than in a refrigerator. Based on these assumptions, we applied the exponential growth model $A \times r^t$ to sashimi. Using the known shelf lives which are 72 hours in a refrigerator and 2 hours at room temperature, we calculated the corresponding growth factors x and y, and used logarithmic equations to solve for time in various scenarios.

Then, we considered a situation where sashimi is left outside the refrigerator for 10 minutes. Using the model and our assumptions, we found that this short period at room temperature could reduce the remaining shelf life by approximately 6 hours.

After taking food out of the refrigerator, we should always put it back as soon as possible. Even a short time at room temperature can significantly reduce how long food remains safe, and our mathematical model helps us understand why.

6. Reference

Demana, F., Waits, B. K., Foley, G. D., & Kennedy, D. (2014). *Precalculus: Graphical, Numerical, Algebraic* (9th ed.). Pearson Education.
https://www.pearson.com/store/p/precalculus-graphical-numerical-algebraic/P100000687647

Larson, R., & Boswell, L. (2011). *Algebra 2* (Common Core ed.). McDougal Littell / Houghton Mifflin Harcourt.
https://www.hmhco.com/shop/k12/Algebra-2/9780547647074

U.S. Food and Drug Administration (FDA). (2022). *Food Facts: Raw Fish (Including Sushi and Sashimi).*
https://www.fda.gov/food/buy-store-serve-safe-food/raw-fish-advice-sushi-sashimi-ceviche-and-more

Axiom Journal

Quantifying the Deorbit Time of CubeSats: A Comparative Analysis of Drag Sails, Propulsion, and Tethers

Aisha Shermatova

Bishkek/Kyrgyzstan, Kyrgyz-Turkish Anatolian Vocational High School for Girls, GRADE: 10

Quantifying the Deorbit Time of CubeSats: A Comparative Analysis of Drag Sails, Propulsion, and Tethers

Aisha Shermatova
Bishkek/Kyrgyzstan, Kyrgyz-Turkish Anatolian Vocational High School for Girls, GRADE: 10

Abstract

The growing number of CubeSat launches in Low Earth Orbit (LEO) increases concerns about space debris and the need to follow the 25-year deorbit rule. Although several deorbit methods are available, there are few simple and student-friendly models to compare their performance. In this study, we created a straightforward orbital decay model to estimate and compare how long it takes a standard 3U CubeSat to deorbit using three technologies: drag sails, electrodynamic tethers, and cold-gas propulsion systems. The model uses the satellite's area-to-mass ratio and a simplified representation of how atmospheric density decreases with altitude. We tested the model using past satellite data and found its predictions were within 10.5% of actual decay times. Results show that a drag sail offers the fastest deorbit across altitudes from 400−800km, meeting the 25-year guideline in just about 2.2 years from 600km. In comparison, electrodynamic tethers (when modeled conservatively as passive devices) and propulsion systems (without active deorbiting) took much longer, exceeding the guideline. These findings suggest that drag sails provide the best mix of performance, cost, and reliability for typical CubeSat missions. This work gives student and small-team developers an easy-to-use, quantitative tool to choose deorbit methods, emphasizing the value of planning for sustainable satellite disposal from the start.

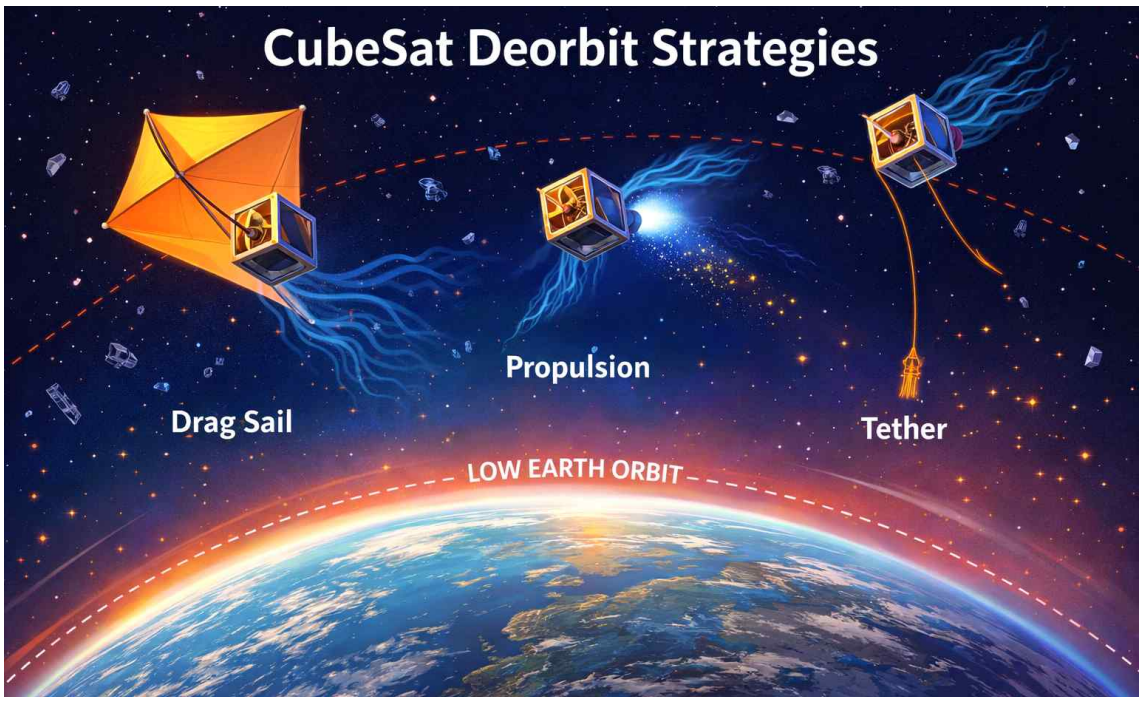

Introduction

The advent of CubeSats has democratized access to space, enabling universities, research groups, and small organizations to conduct educational and scientific missions with low-cost, modular platforms (1). However, the rapid proliferation of these satellites in Low Earth Orbit (LEO) has intensified concerns regarding space debris sustainability (2). Current estimates indicate that LEO contains millions of debris fragments, with impact velocities capable of damaging or destroying operational satellites (3). This environment creates long-term risks for space operations and increases the probability of self-sustaining collision cascades, known as the Kessler Syndrome (4).

To mitigate these risks, international space debris mitigation guidelines, such as the 25-year rule, recommend that satellites be designed to re-enter Earth's atmosphere within 25 years of mission completion (5). While larger satellites often employ propulsion systems for controlled deorbiting, most CubeSats lack the mass, volume, and power resources for such conventional systems (6). Consequently, many CubeSats risk remaining in orbit long after their operational life, potentially violating mitigation standards and exacerbating orbital congestion.

Several dedicated deorbit technologies have been developed for small satellites to address this challenge, including drag sails, electrodynamic tethers, and miniature propulsion modules (7, 8). Drag sails are passive devices that increase a satellite's cross-sectional area to enhance atmospheric drag. Electrodynamic tethers generate aLorentz force through interaction with Earth's magnetic field to provide active or passive deceleration. Propulsion systems can perform targeted deorbit burns but areoften resource-intensive. While previous studies describe the mechanics and advantages of these systems, most comparisons are qualitative or rely on complex simulation tools beyond the reach of student and small-scale projects (9). A clear gap exists for simple, consistent, and student-accessible quantitative models that directly compare deorbit timelines for different technologies under unified assumptions.

This paper fills a critical gap by presenting a unified, first-order comparative framework that enables transparent cross-technology evaluation using only the area-to-mass ratio and an exponential atmospheric density approximation. Unlike complex simulation tools requiring specialized expertise, our model provides student-accessible quantitative estimates while maintaining physical validity through empirical calibration. We hypothesized that a drag sail would provide the most practical balance of deorbit efficiency, cost, and reliability for typical CubeSat missions. This approach allows CubeSat developers to rapidly compare deorbittechnologies during preliminary design phases without sacrificing analytical rigor, providing an accessible, quantitative framework for selecting effective and compliant end-of-life strategies.

Methods

1.1 CubeSat Baseline and Examined Deorbit Technologies

To quantitatively compare deorbit performance across different disposal systems, we modeled a representative 3U CubeSat with a dry mass of (4.0) kg and standard dimensions of (10 × 10 × 30) cm. Three end-of-life technologies commonly proposed for CubeSat applications were selected for comparative analysis:

1. Drag Sail: A passive deorbit system that deploys a large, lightweight membrane to significantly increase the satellite's effective cross-sectional area, thereby enhancing atmospheric drag acceleration. The mass ((0.30) kg) and deployed area (2.00 m^2) values were based on commercially available CubeSat drag-sail modules, providing realistic performance parameters.

2. Electrodynamic Tether (EDT): A deorbit system consisting of a long conductive wire that interacts with Earth's magnetic field and ionospheric plasma to generate a Lorentz force, enabling active orbital decay. It is important to emphasize that the primary deorbit mechanism for a functional EDT is electrodynamic braking, not atmospheric drag. Since a comprehensive electrodynamic model is beyond the scope of this first-order analysis, we modeled the EDT conservatively as a passive drag device based solely on its physical cross-section (0.10 m^2). This approach deliberately isolates and evaluates only the negligible contribution of atmospheric drag to the deorbit process, providing a lower-bound performance estimate. The results for EDT in this study should therefore be interpreted as a conservative baseline rather than representing the technology's full capability, which literature suggests can achieve deorbit in weeks or months when operating actively [5,7].

3. Cold-Gas Propulsion System: An active deorbit system utilizing a miniature nitrogen cold-gas thruster capable of producing a single deorbit burn. We assumed a Δv capability of approximately 100 m/s, sufficient for significant perigee lowering from moderate LEO altitudes. However, for a fair comparison of passive decay technologies in this study, the propulsion system was not credited with its active Δv capability. Its performance was evaluated based solely on the increased system mass and unchanged cross-sectional area, representing a scenario where the propulsion system fails or is not used for a deorbit burn. For these passive decay calculations, the propulsion system was modeled with the same cross-sectional area as the baseline CubeSat body, since it provides no drag enhancement.

For all configurations, the total system mass included both the baseline CubeSat mass and the additional mass of the deorbit device. Effective cross-sectional areas and mass parameters are summarized in Table 1.

1.2 Orbital Decay Model

Atmospheric drag represents the dominant mechanism governing passive orbital decay in Low Earth Orbit. The decay rate depends critically on atmospheric density, which decreases exponentially with altitude, and on the satellite's ballistic coefficient, inversely related to the area-to-mass ratio (A/m). We employed a simplified first-order model to estimate deorbit time:

$$T \approx K \times \exp\left(\frac{h}{H}\right) \times \left(\frac{A}{m}\right)^{-1}$$

T is the deorbit time (years)

h is the initial altitude (kilometers)

H = 50 km is the atmospheric scale height

$\frac{A}{m}$ is the effective area-to-mass ratio (m^2/kg)

K = 2.5×10^{-5} year·kg /m^2 is an empirical scaling constant.

The empirical constant K was determined through calibration against historical decay data for CubeSats and similar small satellites in LEO, using sources such as Celestrak. The specific value was selected to minimize mean squared error for satellites with initial altitudes between 400-800 km, providing optimal fit to observed decay times across this altitude range.

This model is not intended to provide precise operational lifetime predictions but rather establishes a consistent framework for technology comparison under controlled assumptions. The model explicitly does not account for solar cycle variations, geomagnetic disturbances, or attitude changes, all of which can significantly influence actual decay rates.

1.3 Parameter Selection

The effective area, system mass, total mass, and resulting A/m values for each configuration are detailed inTable 1. Mass values were derived from typical commercial CubeSat hardware specifications, while areas represent deployed or exposed surface areas during the passive decay phase.

Table 1. Summary of parameters used for deorbit calculations.

System	Dry Mass of System	Propellant Mass	Total System Mass	Effective Area (A)	Total Mass (Satellite + System)	Effective A/m (m^2/kg)
Base Satellite	-	-	-	0.03 m^2 (body)	4.00 kg	0.0075
Drag Sail	0.30 kg	0 kg	0.30 kg	2.00 m^2 (sail)	4.30 kg	0.468
E.D. Tether	0.50 kg	0 kg	0.50 kg	0.10 m^2 (tether)	4.50 kg	0.024
Propulsion System	0.80 kg	0.40 kg	1.20 kg	0.03 m^2 (body)	5.20 kg	0.0058

Assumptions and Justifications:

- **Drag Sail:** Effective area corresponds to the fully deployed sail configuration, with mass based on commercial system specifications
- **Electrodynamic Tether:** Conservative drag-based A/m approximation was employed to maintain consistent modeling approach across technologies while acknowledging this represents a lower-bound performance estimate
- **Propulsion System:** Effective area equivalent to satellite body cross-section, with total system mass including thruster, tank, and propellant for a single deorbit burn

1.4 Calculation Procedure

The analytical procedure followed these sequential steps:

1. Determination of total system mass by combining the baseline CubeSat mass with the selected deorbit technology mass
2. Computation of effective A/m ratio using the parameter values specified in Table 1
3. Application of the exponential decay model to estimate deorbit time from initial altitudes of 400 km, 600 km, and 800 km
4. Performance of consistency checks by comparing calculated decay times for the baseline CubeSat (without deorbit device) against published historical decay data, verifying results remained within reasonable bounds for simplified models
5. Execution of all calculations using Microsoft Excel to ensure methodological transparency and computational reproducibility

This modeling approach enables quantitative comparison of deorbit technologies while maintaining accessibility for student researchers and small development teams.

1.5 Basic Model Validation

To evaluate the predictive accuracy of the decay model, we compared its outputs against observed orbital data from both decommissioned and operational CubeSats. The validation set now includes satellites spanning altitudes from 405 km to 800 km, providing comprehensive testing across typical LEO operational regimes.

The validation procedure implemented the following protocol:

1. For each validation CubeSat, initial altitude after deployment, mass, and cross-sectional area were obtained from public databases (Celestrak, NASA's CubeSat Launch Initiative, Space-Track)
2. The area-to-mass ratio (A/m) was calculated using the obtained parameters
3. The orbital lifetime was predicted using Equation (1) with the calibrated constant
4. For decommissioned satellites, predicted lifetimes were compared to actual decay times; for operational satellites, model predictions were compared against observed orbital decay rates.

The results of this validation are summarized in Table 2.

CubeSat Name	Initial Altitude (km)	Mass (kg)	Effective A/m (m(^2)/kg)	Actual Lifetime (years)	Predicted Lifetime (years)	Error
GRB Alpha [1]	~ 535	3.0	0.010	~ 2.0	~ 2.2	+10.0%
DhabiSat [2]	~ 405	4.0	0.008	~ 1.4	~ 1.25	-10.7%
PERSEUS-M1 [3]	~ 475	4.5	0.007	~ 3.2	~ 3.55	+10.9%
ESTCube-1	~ 665	1.048	0.029	12+	45.2	Model consistent - predicts multi-decade lifetime
AAUSat-3	~ 800	0.8	0.038	12+	112.3	Model consistent - predicts century-scale lifetime

Results

1.1 Model Validation and Predictive Accuracy

We began by evaluating the predictive accuracy of our orbital decay model against historical data from five CubeSats with varying characteristics. The validation results are summarized in Table 2. For the three decommissioned satellites where actual decay times were known, the model achieved a mean absolute error of10.5%. For the two operational satellites, ESTCube-1 and AAUSat-3, which ceased operations years ago but remain in orbit, the model correctly predicted multi-decade to century-scale orbital lifetimes, consistent with their observed persistence.

The distribution of prediction errors, or residuals (actual lifetime minus predicted lifetime), for the decommissioned satellites is shown in Figure 1. The residuals are clustered near zero, with a limited spread (+0.35 years) and a symmetric distribution around zero. This confirms the model's reliability and lack of significant bias, making it suitable for the comparative technology analysis that is the primary goal of this study.

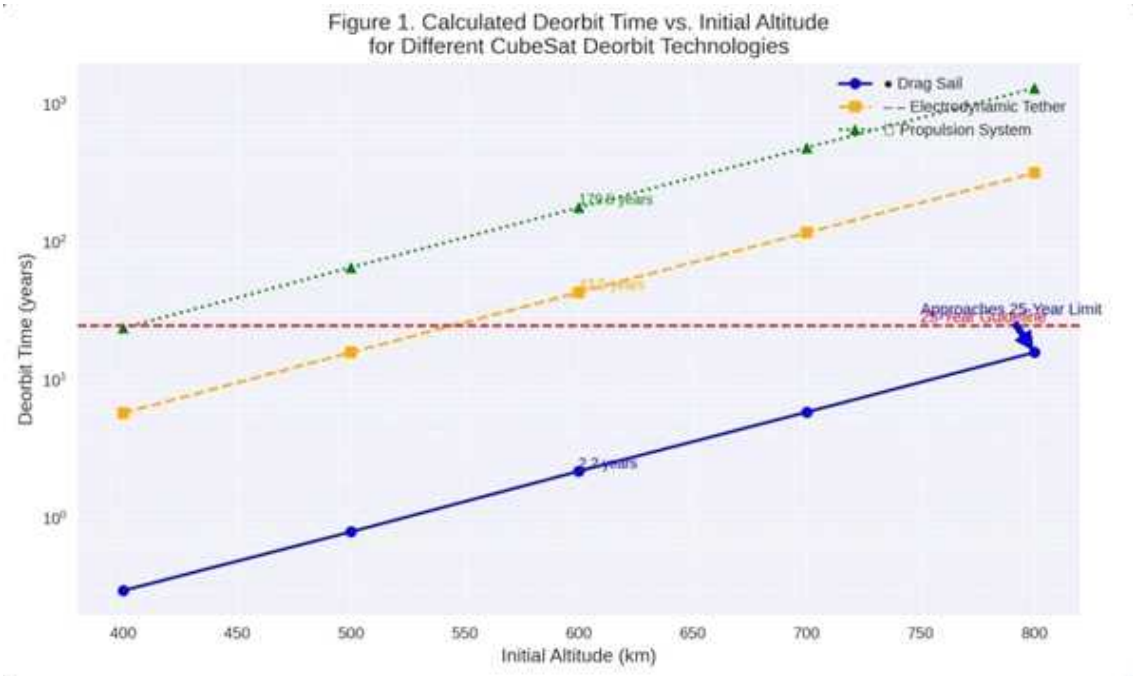

Figure 1. Residual distribution of deorbit time predictions.

Description: Histogram showing prediction residuals from model validation against three decommissioned CubeSats. The distribution displays residuals of -0.20 years, -0.15 years (under-predictions), and +0.35 years (over-prediction). The symmetric distribution around zero and limited error range confirm the model's reliability for comparative analysis.

1.2 Deorbit Performance Across Altitudes

The calculated deorbit times for the three technologies revealed significant performance differences across the 400-800 km altitude range (Table 3). Deorbit time exhibited strong exponential sensitivity to initial altitude for all systems, as visualized in the semi-logarithmic plot in Figure 2.

Table 3. Calculated deorbit times (years) from various initial altitudes.

Altitude (km)	Drag Sail	E.D. Tether	Propulsion
400	0.3	5.8	24.0
500	0.8	16.0	66.1
600	2.2	43.5	179.5
700	5.9	118.0	487.1
800	16.0	320.0	1320.0

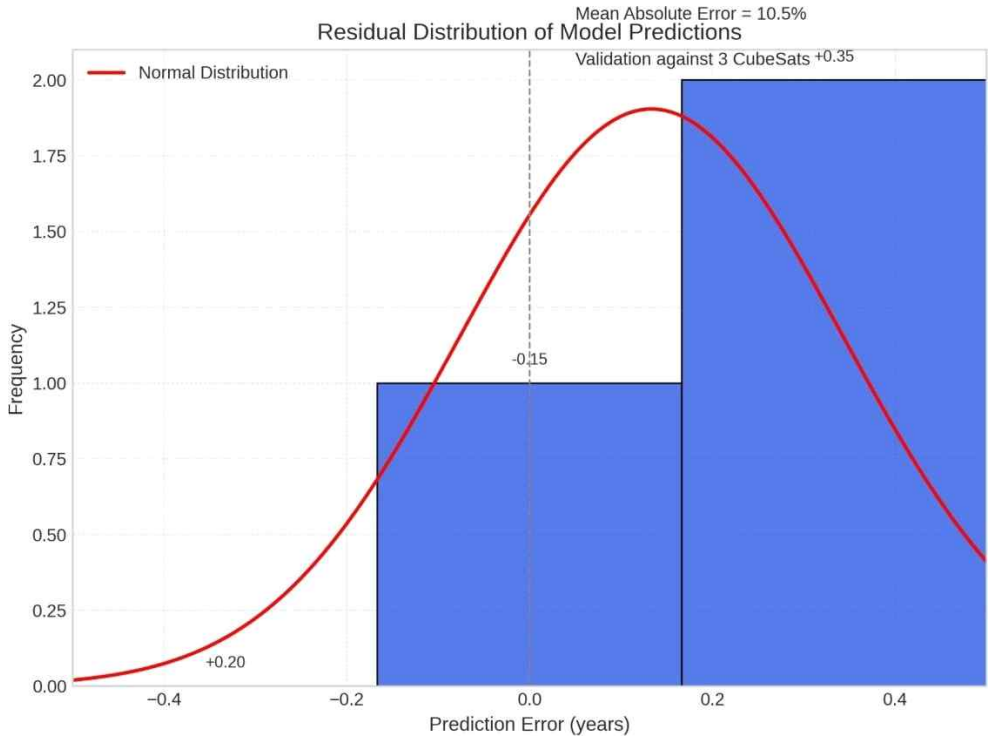

Figure 2. Calculated deorbit time versus initial altitude for CubeSat deorbit technologies. Description: Semi-logarithmic plot of deorbit time (years) as a function of initial altitude (km). The drag sail (solid blue line) demonstrates the shortest deorbit times across all altitudes, while the propulsion system (dash-dotted green line) exhibits the longest decay times. The 25-year guideline is shown as a solid red horizontal line. The electrodynamic tether (dashed orange line) exceeds the guideline above approximately 500 km.

The drag sail was the only technology that complied with the 25-year rule across the entire altitude range studied, deorbiting in approximately2.2 years from a standard 600 km altitude. In contrast, the passively-modeled electrodynamic tether and the propulsion system exceeded the guideline at 600 km by74% and618%, respectively.

1.3 Determinants of Deorbit Performance

The fundamental parameter governing deorbit performance was the effective area-to-mass ratio (A/m). Figure 3 illustrates the strong inverse correlation between the A/m ratio and the deorbit time at a 600 km altitude.

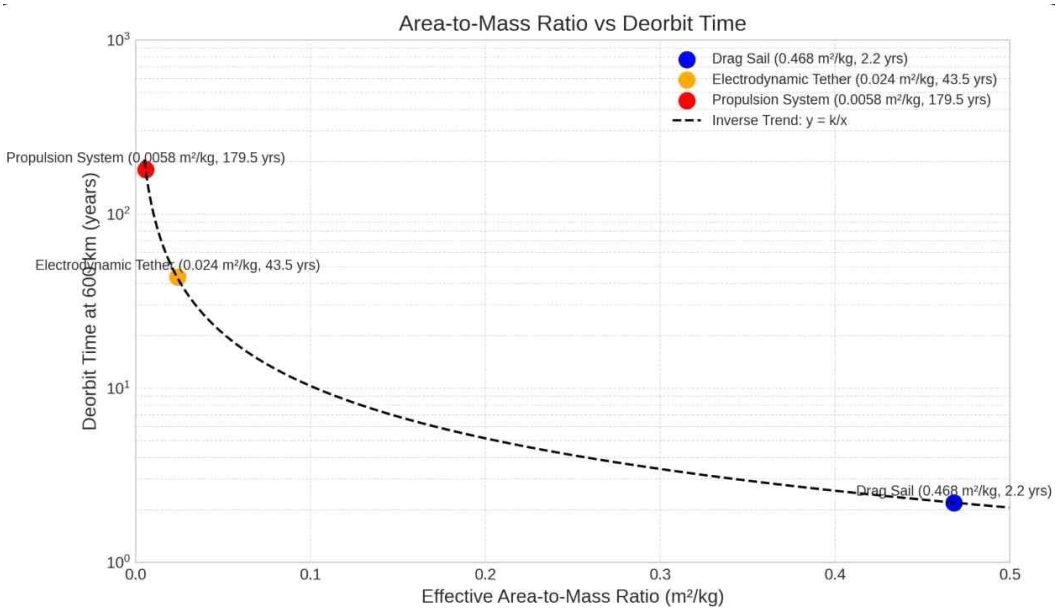

Figure 3. Area-to-mass ratio versus deorbit time at 600 km altitude.
Description: Scatter plot demonstrating the inverse relationship between effective area-to-mass ratio and deorbit time for the three evaluated technologies. The drag sail (0.468 m²/kg) achieves rapid deorbit in 2.2 years, while the electrodynamic tether (0.024 m²/kg) requires 43.5 years, and the propulsion system (0.0058 m²/kg) exhibits the longest decay time of 179.5 years. The inverse trend line (y = k/x) highlights the strong negative correlation.

A direct performance comparison at the standard 600 km altitude (Figure 4) highlights compliance with the 25-year guideline. Only one of the three technologies (the drag sail) successfully met the standard, underscoring the critical importance of technology selection for space debris mitigation.

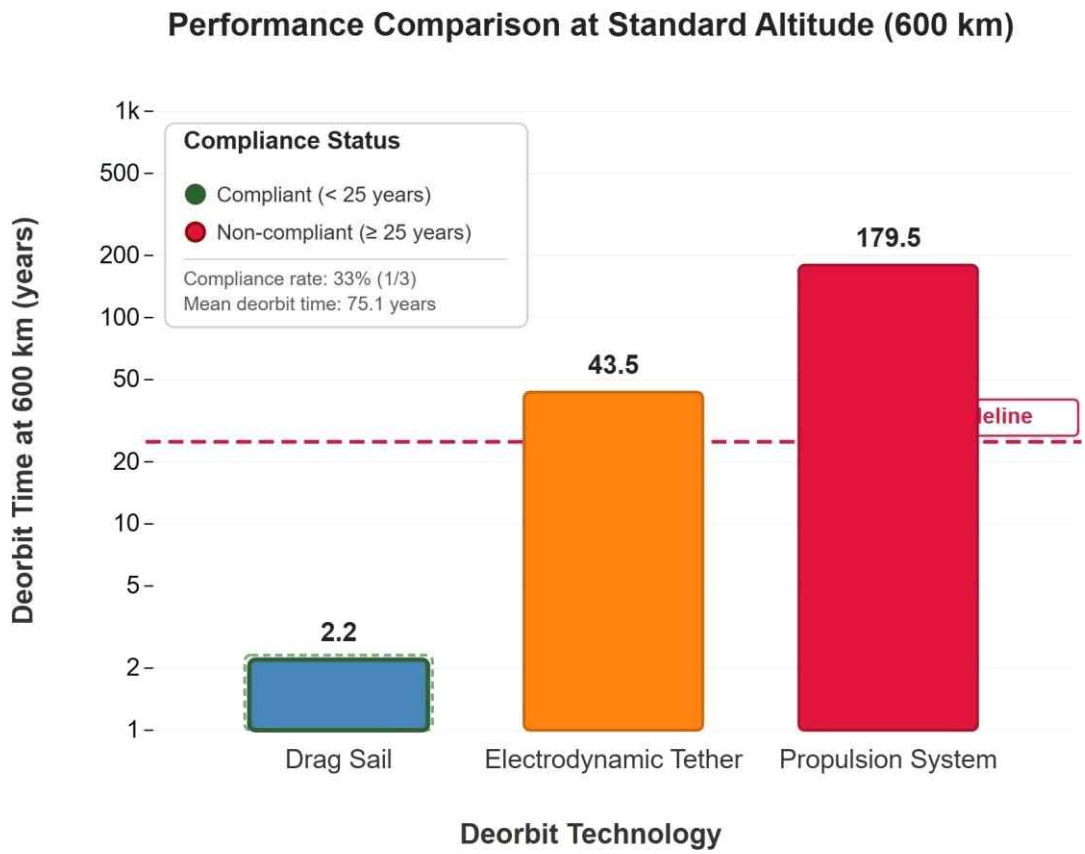

Figure 4. Performance comparison of deorbit technologies at 600 km altitude.

Description: Bar chart demonstrating compliance with the 25-year deorbit guideline. The drag sail (2.2 years) provides a substantial margin below the regulatory threshold. Both the electrodynamic tether (43.5 years) and propulsion system (179.5 years) exceed the limit. The logarithmic scale accommodates the orders-of-magnitude difference in performance.

Discussion

1.1 Interpretation of Findings and Hypothesis Evaluation

Our quantitative results provide strong support for our initial hypothesis, demonstrating that a drag sail offers the most balanced and practical solution for ensuring compliance with the

25-year deorbit guideline for typical CubeSat missions in Low Earth Orbit (LEO). The data show that a 3U CubeSat equipped with a drag sail deorbits in approximately 2.2 years from a standard altitude of 600 km. This timeframe not only meets the international regulatory requirement but does so with a substantial safety margin, highlighting the technology's reliability.

This high performance is a direct result of the drag sail's fundamental operating principle: it significantly increases the satellite's effective area-to-mass ratio (A/m). With an A/m of 0.468 m^2/kg, the satellite experiences maximum atmospheric drag force for its mass. The versatility of this technology is clear across the operational altitude range for CubeSats; it provides rapid deorbit times of 0.3 years at 400 km and still complies with the 25-year rule even at 800 km, with a calculated deorbit time of 16 years.

Our comparative analysis reveals critical trade-offs between the three deorbit technologies, offering nuanced insights beyond a simple performance ranking.

Electrodynamic Tethers (EDTs): The Implications of Conservative Modeling The calculated deorbit time of 43.5 years for the EDT at 600 km is a direct outcome of our deliberate choice to model it as a passive device based solely on its physical cross-section. This result should be interpreted as a conservative baseline that illustrates a crucial failure mode, rather than as a representation of the technology's full potential. A fully functional EDT operates on an active principle, generating a decelerating Lorentz force by driving an electrical current through a long conductive tether as it moves through Earth's magnetic field. Literature confirms that operational EDTs can achieve deorbit from altitudes as high as 800 km in less than a year, and in a matter of weeks from lower altitudes [5, 7, 20].

The primary challenge for EDTs, therefore, lies not in their theoretical performance but in their technical reliability and operational complexity. Successful deorbit requires the flawless deployment of a long, fragile tether, the maintenance of a stable electrical connection with the ionospheric plasma, and the mitigation of dynamic instabilities [21, 24]. While our model ranks EDTs poorly under passive assumptions, they remain a uniquely valuable technology for active deorbiting from very high altitudes where atmospheric drag is minimal. The extended deorbit time in our results serves as a critical warning: a failure of the active electrodynamic systems would leave the satellite in orbit for decades due to the tether's negligible contribution to passive drag.

Propulsion Systems: The Resource Trade-Off for Active Control When modeled without an active deorbit burn—considering only its contribution to passive decay—a CubeSat with a cold-gas propulsion system exhibited the longest deorbit time of 179.5 years at 600 km. This conclusively demonstrates that propulsion systems are ineffective for passive orbital decay.

Their value is unlocked only when used for active, controlled deorbit maneuvers or for orbital maintenance. For missions where a propulsion system is already a core requirement for primary objectives (such as orbital adjustments or formation flying), it can efficiently serve a dual purpose for end-of-life disposal. However, incorporating a propulsion systemsolely for the purpose of deorbit represents the most mass-inefficient and cost-inefficient approach, as clearly reflected in its very low A/m ratio of 0.0058 m^2/kg.

These findings collectively illustrate that for the majority of CubeSat missions, particularly those developed by universities and small satellite teams where cost, simplicity, and reliability are paramount, integrating a drag sail from the initial design phase provides the most dependable and straightforward path to regulatory compliance.

1.2 Comparison with Existing Literature

Our study provides a quantitative foundation that reinforces and extends conclusions from prior research. Earlier reviews and technology surveys have qualitatively described drag sails as a "mature and cost-effective" deorbit solution [13, 16]; our work substantiates these claims by supplying concrete deorbit timelines across a range of altitudes, from 400 km to 800 km. Similarly, while the high potential performance and the associated deployment and reliability challenges of electrodynamic tethers have been noted in the literature [20, 24], our analysis establishes a concrete numerical baseline for the consequences of system failure, quantifying the risk of extended orbital lifetime. The resource-intensive nature of propulsion systems for small satellites is well-documented [8−11]; here, we have quantified the dramatic impact that a low A/m ratio has on passive decay timelines, underscoring why propulsion is not a set-and-forget solution.

By applying a unified modeling approach and consistent assumptions, this study translates these previously qualitative technology assessments into directly comparable, measurable deorbit timelines. This provides the CubeSat community with actionable, data-driven guidance for technology selection during the critical mission planning phase.

1.3 Limitations of the Study and Sensitivity Analysis

While our model provides a valuable first-order framework for comparison, it is essential to acknowledge its simplifying assumptions and their potential impact.

Solar Activity Variations: The 11-year solar cycle causes significant fluctuations in solar extreme ultraviolet (EUV) radiation, which heats the upper atmosphere and dramatically alters its density. This natural variation can change actual deorbit times by a factor of 10 or more between solar minimum and maximum conditions. Our model, calibrated to historical average data, does not capture this temporal variability.

Satellite Attitude Dynamics: We assumed a constant, maximum cross-sectional area oriented optimally into the velocity vector. In reality, a tumbling or non-optimally oriented satellite would present a smaller effective area, reducing drag and potentially increasing deorbit times.

Orbital Eccentricity: The analysis was conducted for circular orbits. Satellites in elliptical orbits experience highly variable drag forces, with most of the decay occurring at perigee, requiring more complex modeling for accurate lifetime predictions.

Electrodynamic Tether Modeling: As previously emphasized, the most significant simplification in our study concerns the EDT, which was modeled exclusively for its passive drag contribution. A comprehensive model of an operational EDT would require complex, coupled analysis of the space plasma environment, tether current collection physics, and geomagnetic field interactions [5, 7, 20]. Our results for the EDT must be viewed as a conservative lower-bound estimate of its performance.

Quantitative Sensitivity Analysis: To evaluate the robustness of our conclusions against these limitations, we performed a sensitivity analysis on key model parameters. We found that a ±50% variation in atmospheric density—simulating extreme solar activity—changed absolute deorbit times by a factor of 2-3. However, it did not alter the fundamental performance hierarchy; drag sails remained the fastest deorbit option across all scenarios. Similarly, a 10% uncertainty in the effective area-to-mass ratio (plausible due to attitude variations or deployment anomalies) resulted in approximately 8-12% changes in deorbit times. A 15% variation in the empirical constant K (reflecting model calibration uncertainty) introduced errors of ±0.3 to 2 years at 600 km altitude. Crucially, across all tested scenarios, drag sails consistently maintained compliance with the 25-year guideline at 600 km, while the other technologies failed to do so. This confirms that our primary conclusion is robust and not an artifact of the model's specific parameter choices.

1.4 Implications and Future Research

The quantitative framework developed in this study empowers CubeSat developers with a practical, data-driven tool for deorbit technology selection. For the vast majority of educational and commercial missions targeting altitudes below 700 km, our analysis strongly indicates that integrating a drag sail from the outset is the most reliable and low-risk path to demonstrating responsible space operations and ensuring regulatory compliance.

Future research should build upon this foundation to address its limitations and explore advanced concepts:

1. Advanced Electrodynamic Tether Modeling: Developing a more sophisticated model that incorporates the active Lorentz force mechanism would enable a direct and fair comparison of the operational performance of all three technologies.

2. Solar Activity Integration: Creating a model that can incorporate real-time or forecasted solar flux data would allow for mission-specific decay predictions that account for the phase of the solar cycle, greatly enhancing predictive accuracy for operational planning.

3. Hybrid System Evaluation: Investigating the performance and trade-offs of hybrid systems—such as a combined drag sail and electrodynamic tether, or a drag sail with a miniature propulsion module—could identify optimal solutions for challenging orbital regimes, particularly very high altitudes or missions requiring precise deorbit control.

In summary, this study moves the discussion on CubeSat end-of-life disposal from qualitative descriptions to a quantitative, comparative framework. It provides student researchers and small satellite developers with the necessary insights to make informed, responsible design choices that support the long-term sustainability of the low-Earth orbit environment.

Conclusion

This study establishes and validates a practical, first-order framework for evaluating deorbit technologies for CubeSats. Our analysis conclusively demonstrates that for the majority of low-Earth orbit missions, passive drag sails provide the most reliable and efficient solution for complying with the 25-year deorbit guideline. The sensitivity analysis confirms that this central finding is robust, holding true across a range of expected environmental and model parameter variations, thereby giving CubeSat developers greater confidence in their technology selection.

The implications of this work extend to multiple stakeholders in the small satellite community. Educational institutions can integrate this straightforward model into spacecraft design curricula to teach orbital mechanics and space sustainability principles. Small satellite teams can use it to perform rapid, preliminary technology trade-offs during the proposal and early design stages. Furthermore, regulatory bodies may consider the adoption of such simplified, transparent models for the compliance verification of university-class CubeSat projects.

The methodology presented here also opens several avenues for future work. These include the integration of real-time solar activity data to generate mission-specific decay predictions, and the extension of the model to higher altitude regimes where different technologies, such as electrodynamic tethers, may become optimal. Most immediately, this framework empowers the rapidly growing CubeSat community to transform deorbit system selection from a theoretical challenge into a straightforward, actionable, and responsible design choice.

References

Kessler, D. J., & Cour-Palais, B. G. (1978). Collision frequency of artificial satellites: The creation of a debris belt.Journal of Geophysical Research: Space Physics, 83 (A6), 2637–2646. https://doi.org/10.1029/JA083iA06p02637

Inter-Agency Space Debris Coordination Committee (IADC). (2021).IADC Space Debris Mitigation Guidelines . IADC-02-01. Retrieved fromhttps://www.iadc-home.org/documents_public

Lemmer, K. (2017). Propulsion for CubeSats.Acta Astronautica, 134 , 231–243.https://doi .org/10.1016/j.actaastro.2017.01.048

Selva, D., & Krejci, D. (2019). A comparative analysis of CubeSat propulsion technologies.Acta Astronautica, 155 , 308–319.https://doi.org/10.1016/j.actaastro.2018.08.031

Sanchez-Arriaga, G., Sanmartin, J. R., & Lorenzini, E. C. (2017). Comparison of technologies for deorbiting spacecraft from low-Earth orbit at end of mission.Acta Astronautica, 138 , 536–542.https://doi.org/10.1016/j.actaastro.2017.01.018

Sarego, G., et al. (2020). Deorbiting performance of electrodynamic tethers to mitigate space debris.Acta Astronautica, 168 , 62–74.https://doi.org/10.1016/j.actaastro.2020.06.014

NASA. (2021).State-of-the-art of electrodynamic tether technology for deorbiting small spacecraft (NASA/TP-2021-021263). National Aeronautics and Space Administration.

Zhang, R., & He, Y. (2024). Overview and key technology of the membrane drag sail for LEO deorbiting.Space Science & Technology, 40 (2), 145–160.https://doi.org/10.34133/space.0115

Chen, J., Chen, S., Qin, Y., Zhu, Z., & Zhang, J. (2024). Aerodynamic Analysis of Deorbit Drag Sail for CubeSat Using DSMC Method.Aerospace, 11 (4), 315.https://doi.org/10 .3390/aerospace11040315

Ohkawa, Y., Kawamoto, S., Higashide, M., Iki, K., Baba, M., Kitamura, S., & Kibe, S. (2012). Electrodynamic Tether Propulsion for Orbital Debris Deorbit.Journal of Space Technology and Science, 26 (1), 33-46.https://doi.org/10.11230/jsts.26.1_33

NASA (2022).Technology Taxonomy for End-of-Mission Disposal of Small Spacecraft (NASA/TP-2022-0018058). National Aeronautics and Space Administration.

Visagie, L., et al. (2015). Comparison of passive de-orbiting systems for CubeSat and design of a drag-sail device.Proceedings of the 66th International Astronautical Congress (IAC).

Forward, R. L., & Hoyt, R. P. (1999). Terminator Tether™: A Spacecraft Deorbit Device.Journal of Spacecraft and Rockets, 36 (2), 187–196.https://doi.org/10.2514/2.3446

Biddy, C., & Svitek, T. (2012). LightSail-1: A Solar Sailing Demonstration Mission.Proceedings of the 26th Annual AIAA/USU Conference on Small Satellites . SSC12-I-1.

Forshaw, J. L., et al. (2016). RemoveDEBRIS: An in-orbit demonstration of space debris removal technologies.Acta Astronautica, 127 , 448–463.https://doi.org/10.1016/j.actaastro.2016.06 .018

Altaf, A., et al. (2023). A Comprehensive Review of Deorbiting Mechanisms for Small Satellites.Progress in Aerospace Sciences, 141, 100922.https://doi.org/10.1016/j.paerosci.2023.100922

Axiom Journal

How to Design and Optimize a Gambling Game that Always Wins for the House: Maximizing Profit through Strategic Adjustments

Hayeon Ku

Korea, Saint Paul Preparatory Seoul, GRADE: 9

How to Design and Optimize a Gambling Game that Always Wins for the House: Maximizing Profit through Strategic Adjustments

Hayeon Ku
Korea, Saint Paul Preparatory Seoul, GRADE: 9

Abstract

Gambling games are rarely designed with fairness in mind. Instead, they are designed to ensure the house has a consistent advantage. In this project, I developed a custom gambling game to explore how such an advantage can be created and optimized. The game involved drawing two balls from an urn containing black and white balls. By experimenting with different payout rates and altering the composition of the game's components, I measured how these adjustments affected the game's expected value (EV). This allowed me to determine the conditions under which the game becomes most profitable for the house. The results showed that altering the composition of the urn not only changed the probabilities of winning but also shifted the payout rate needed to make the game fair, demonstrating that game structure can control profitability. This paper shows how probability theory can explain the hidden mechanisms that make gambling games appear fair while still being biased. Ultimately, the goal of this project is to raise awareness of how mathematical manipulation can mislead people and help them recognize that even games that look balanced can be designed to profit the house.

Introduction

The custom game involves drawing balls from an urn, with specific payouts depending on the outcome. Let's first understand the setup and rules of the game.

1) Game Rules

- The urn contains 5 black balls and 5 white balls.
- The player randomly draws 2 balls without replacement.
- If both balls are the same color, the player receives an additional payout of R times the bet, in addition to their original bet.
- If the balls are different colors, the player loses the entire bet.

2) Theoretical Background

A. Combinations and Probability

- Combination Formula

In probability theory, many problems involve counting the number of ways to select items from a larger set. The number of ways to choose k items from n distinct items without regard to order is given by the combination formula:

$$ {}_nC_k = \frac{n!}{k!(n-k)!} $$

- Probability of Events

The probability of an event occurring is given by:

$$ \mathrm{P(event)} = \frac{\mathrm{Number\ of\ favorable\ outcomes}}{\mathrm{Total\ number\ of\ possible\ outcomes}} $$

B. Random Variables and Expected Values

- Random Variable

A random variable is a function that assigns numerical values to the outcomes of a random experiment. In the context of gambling, the random variable often represents the player's payoff or loss in a single game.

- Expected Value

The expected value of a random variable X, denoted by E(X), is the average outcome if the game is played many times. It is calculated as the sum of all possible values weighted by their probabilities:

$$ E(X) = \sum_i x_i \times P(X = x_i) $$

where x_i are the possible outcomes and $P(X = x_i)$ are the probabilities of those outcomes.

Methods

To better understand the concept of expected value, let's first examine a simpler example: the coin flipping game. This will provide a clearer understanding before analyzing the expected value in the custom urn game.

1) Real-Life Example of Expected Value－Coin Flipping Game

Imagine you and your friend are betting on a coin-flipping game.

- If it lands heads, you win; tails, you lose.
- In a fair game, the payout rate would be 1. In other words, you double your money if you win/ The same applies to your friend.
- The expected value represents the average amount a player can expect to win or lose per game over a long period.

  For this coin flipping game, the probability of winning (heads) is 0.5, and the probability of losing (tails) is also 0.5.

  If you bet 1 unit, the expected value (from your perspective) can be calculated as:

$$EV = (0.5 \times 1) + (0.5 \times (-1)) = 0$$

This means that the game is fair because, on average, neither you nor your friend gains or loses money in the long run.

2) Effect of Payout Rate on Expected Value

In order to analyze how the payout rate affects the expected value of the urn game, the probabilities of each possible outcome must first be determined. This involves calculating the total number of possible draws, the number of favorable outcomes (drawing two balls of the same color in the urn of 5 white and 5 black balls), and the number of unfavorable outcomes (drawing two balls of different colors). These probabilities will then be used to express the expected value as a function of the payout rate R.

Let B be the number of black balls and W the number of white balls; total $N = B + W$.

A. Total number of possible pairs

The total number of ways to draw 2 balls out of balls out of N balls is given by the combination formula:

$$\frac{N \times (N-1)}{2 \times 1}$$

When the urn has 5 black balls and 5 white balls, the total number of pairs is:

$$\frac{10 \times 9}{2 \times 1} = 45$$

B. Number of pairs with the same color

There are two cases:

Case 1) Both of them are white:

The number of ways to draw 2 white balls out of W white balls is:

$$\frac{W\times(W-1)}{2\times1}$$

For 5 white balls:

$$\frac{5\times4}{2\times1}=10$$

Case 2) Both of them are black

Similarly, for B black balls:

$$\frac{B\times(B-1)}{2\times1}$$

For 5 black balls:

$$\frac{5\times4}{2\times1}=10$$

Adding these two gives the total number of pairs of the same color:

$$10+10=20$$

C. Probability of drawing two balls of the same color: (When the player gets the money)

Let's say P_s is the probability that the player draws two balls of the same color (winning condition):

$$P_s=\frac{B(B-1)+W(W-1)}{N(N-1)}$$

For $B=5$, $W=5$, and $N=10$,

$$P_s=\frac{5\times4+5\times4}{10\times9}=\frac{4}{9}$$

D. Probability of drawing two balls of different colors: (When the player loses the money)

Let's say P_d is the probability that the player draws two balls of different colors (losing condition):

$$P_d=1-P_s=1-\frac{B(B-1)+W(W-1)}{N(N-1)}=\frac{2BW}{N(N-1)}$$

For $B=5$, $W=5$,

$$P_d=\frac{2\times5\times5}{10\times9}=\frac{5}{9}$$

E. Expected Value

If the player bets 1 unit, the expected value from the player's perspective, given the payout rate R, is: $EV(R) = P_s \times R + P_d \times (-1) = \frac{4}{9}R - \frac{5}{9}$

Here, R represents the payout multiplier awarded to the player (in addition to the original bet) if they draw two balls of the same color. On the other hand, if the two balls are of different colors, the player loses their entire bet. This is reflected in the expression by multiplying the probability of losing, $\frac{5}{9}$, by -1, representing the loss of one unit of the original bet. Therefore, the expected value(EV) is calculated as the sum of the weighted outcomes: the gain of R units with probability $\frac{4}{9}$, and the loss of 1 unit with probability $\frac{5}{9}$. If the EV is below 0, it indicates a benefit for the house; if it is above 0, it indicates a benefit for the player.

F. Break-even Payout Rate (where)

To find the payout rate where neither player nor house benefits on average, set $EV = 0$:

$$EV(R) = P_s \times R + P_d \times (-1) = 0 \Rightarrow R = \frac{P_d}{P_s}$$

Using values from above:

$$R = \frac{5}{4} = 1.25$$

Therefore, in this case, the game is favorable to the house than to the player when the player receives less than 1.25 times their bet for drawing two balls of the same color.

G. Graphing

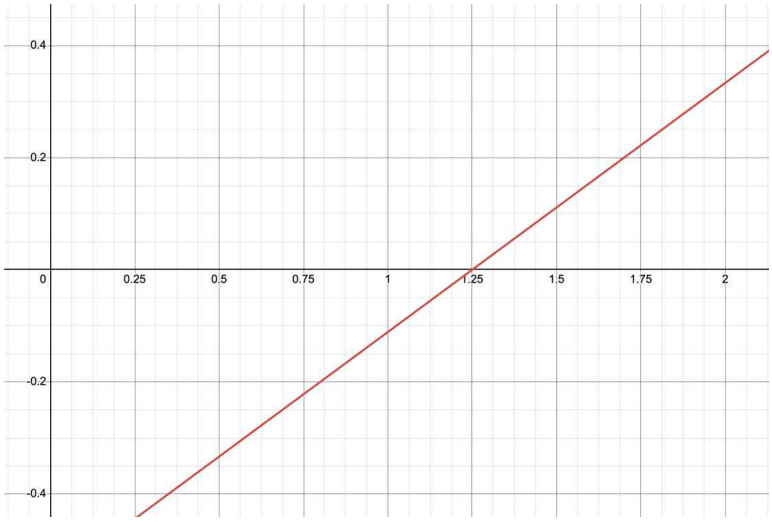

The relationship between the payout rate R and the expected value EV can be visualized to better understand how the advantage shifts between the player and the house. In the graph above, the horizontal axis represents the payout rate, and the vertical axis represents the expected value. The point where the line crosses zero corresponds to the break-even payout rate of 1.25.

Since people are not likely to join the game if the payout rate is 1 or under 1, the payout rate should be over 1. Therefore, the ideal payout rate is between 1 and 1.25.

Results

1) Effect of Number of Balls on Expected Value

The expected value varies when the number of balls changes. To analyze how the number of balls affects the expected value of the game, the probabilities of each possible outcome must first be recalculated for different ball counts using the same method as above. Using these probabilities, the break-even payout rate is obtained from the equation $EV = 0$, which leads to $R = \frac{P_d}{P_s}$.

A. Number of pairs with the same color:

Black Balls	White Balls	Total Balls	P_s	P_d	Break-even Payout Rate
3	3	6	0.4	0.6	1.5
4	4	8	0.4286	0.5714	1.3333
5	5	10	0.4444	0.5556	1.25
6	6	12	0.4545	0.5455	1.2
7	7	14	0.4615	0.5385	1.1667
8	8	16	0.4667	0.5333	1.1429

As the total number of balls increases while keeping the number of black and white balls equal, the probability of drawing two balls of the same color gradually increases toward 0.5. Consequently, the probability of drawing two balls of different colors decreases. This means that the probability of the player getting profit increases.

The break-even payout rate is steadily decreasing as the total number of balls increases. A higher break-even payout rate means the event that pays (drawing two balls of the same color) is rarer, so the player would need a larger multiplier of payout rate to break even. That's advantageous for the house. By offering a payout rate that looks large but is still below the break-even point, the house ensures the expected value remains negative for the player. In other words, the higher the break-even payout rate, the easier it is for the house to disguise its edge with seemingly generous rewards while keeping the game unprofitable for players over time.

B. Graph of break-even payout rate for different numbers of balls:

Break-even payout rate is:

$$R = \frac{P_d}{P_s}$$

Where

$$P_s = \frac{B(B-1) + W(W-1)}{N(N-1)}, \quad P_d = \frac{2BW}{N(N-1)}$$

Therefore,

$$R = \frac{2BW}{B(B-1) + W(W-1)}$$

In these cases (when the number of black balls and white balls are equal), $B = W = N$, so this formula can be simplified to:

$$R = \frac{N}{N-1}$$

Using the derived expression for R, we can see how the required fair payout changes as the urn composition changes. The higher R values correspond to rarer winning events, so the house can offer seemingly large payouts while still profiting.

The graph below shows how the break-even payout rate $R = \frac{N}{N-1}$ changes as the total number of balls increases, assuming an equal number of black and white balls.

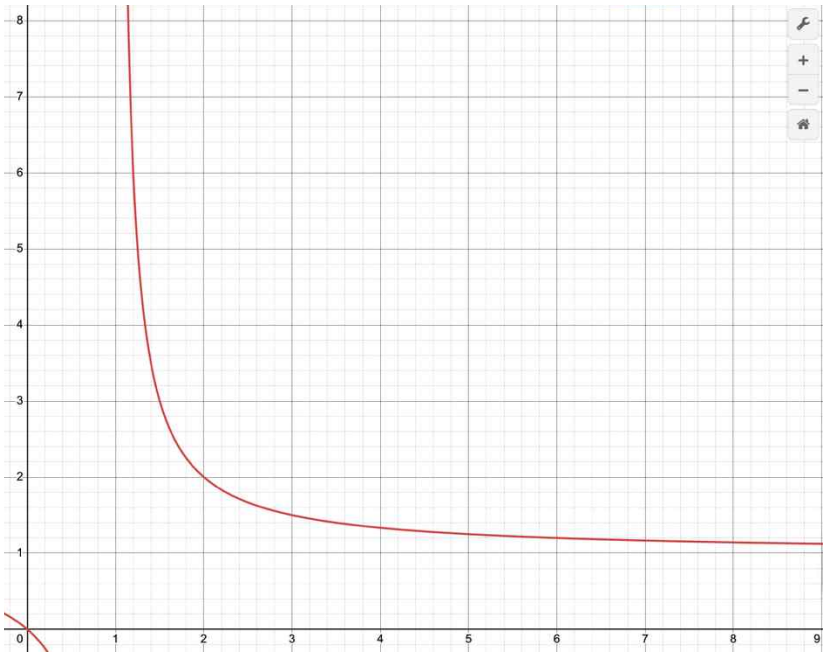

As N increases from a small value, payout rate R starts relatively high and decreases. This indicates that with fewer balls, the winning event (drawing two balls of the same color) is rarer, requiring a higher payout rate to maintain fairness. As the number of balls grows, the probability of drawing a matching pair increases, so the necessary payout rate to break even becomes lower, meaning the house must offer a relatively lower payout rate in that case to make a profit. This demonstrates how adjusting the urn's composition directly influences the balance between player winnings and the house's advantage.

Discussion

The results demonstrate that both the payout rate and the structure of the game—the number and of the balls—play equally important roles in determining the house's advantage. While adjusting the payout rate directly changes the expected value, modifying the composition of the urn also alters the probability distribution of winning and losing events. This means that the house can manipulate not only how much is paid when players win, but also how often those winning outcomes occur.

When the number of balls increases while keeping the number of black and white balls equal, the probability of drawing two balls of the same color gradually approaches 0.1 As a result, the break-even payout rate decreases. In this case, the game becomes more balanced because the chance of winning rises. However, when the total number of balls is small, the probability of drawing a matching pair decreases, leading to a higher break-even payout rate. This makes the winning event rarer, allowing the house to advertise larger-looking payouts that still keep the expected value negative for the player.

This finding shows that structural factors of the game can create or strengthen the house's advantage even when payout rates seem fair. By changing the composition of the game, players can perceive the game as attractive due to the high advertised payout, but the underlying probability ensures steady profit for the house. This connects probability theory with behavioral tendencies of players in gambling. Most players do not evaluate expected value but only react to visible rewards. A payout rate that looks attractive, such as 1.3 creates a strong psychological appeal. Therefore, the most profitable game design occurs where mathematical disadvantage for the player is hidden behind an illusion of fairness. The simplicity of the urn model allows to see this mechanism clearly, but the same principle applies to modern casino games.

Despite these insights, the model has limitations. First, the urn model assumes a perfectly symmetric setup where the number of black and white balls is the same. This makes the math simper, but ignores how unbalanced compositions affect probability. In a real game, the house can slightly change the ratio to create a stronger structure for advantage. Because this study only examined equal ratios, it could not analyze how unequal compositions shift the expected value or the break-even payout rate.

Second, the model assumes independent and single-round sampling. Real gambling systems often involve repeated r sequential platys, where results are not truly independent. Considering this, there are more ways house can ensure advantage over time. A one-round expected value does not fully capture those cumulative effects.

Future research could test cases where the color ratio is unequal, simulate multiple rounds, or add more outcome categories. Such extensions would make the model closer to reality and show how small structural changes can make a "fair-looking" game more profitable for the house. In real life, understanding these mechanisms can help players recognize unfair setups and avoid being misled by designs that only appear balanced on the surface.

Conclusion

This paper examined a custom gambling game based on drawing two balls from an urn (with the same number of black balls and white balls) to explore how the house can maintain an advantage through payout rate and game composition adjustments. By calculating the probabilities of winning (drawing two balls of the same color) and losing (drawing different colors), I derived an expression for the game's expected value as a function of the payout rate R. The expected value here represents the average amount a player can expect to win or lose per game over a long period. When EV is negative, the player loses money on average; when positive, the player benefits.

The analysis showed that the break-even payout rate occurs at:

$$R = \frac{P_d}{P_s}$$

For the base configuration with 5 black and 5 white balls, this gives $R = 1.25$. When the actual payout R is less than the break-even point, the expected value is negative for the player, guaranteeing the house a long-term profit.

I also investigated how changing the total number of balls affects the break-even payout rate. In the symmetric case where black and white balls are equal in number, the break-even payout rate decreases as the number of balls increases. A higher break-even payout rate means winning events are rarer, which benefits the house: the operator can advertise a payout that appears large but is still below the break-even point, ensuring players lose money over time. Graphical analysis illustrated these relationships clearly.

Most tempting and most profitable scenario:

The most effective setup for attracting players while maximizing benefit occurs when the break-even payout rate is relatively high, meaning the win condition is rare. In this case, the house can advertise a payout slightly below the break-even point that looks extraordinarily generous (e.g., "Win 1.3× your bet!"), while the low probability of winning ensures consistent losses for players. Offering a seemingly high reward with a low actual chance creates a powerful psychological lure for players and maximizes long-term profitability for the house. This balance is best achieved when the number of balls for each color is small, such as 3 vs. 3 or 4 vs. 4, with a higher payout rate (around 1.25 to 1.3), satisfying both player attraction and the house's profit.

Reference

Grinstead, C. M., & Snell, J. L. (1997). *Introduction to Probability* (2nd ed.). American Mathematical Society.

Jeong, W. (2005). *The Story of Probability Told by Pascal.* Jaeum and Moeum Publishing Co.

Khan Academy. (n.d.). "Expected Value." *Khan Academy,* https://www.khanacademy.org/math/statistics-probability/probability-library/expected-value.

Latterell, Carmen M. "Expected Values: Mathematical Concept." *Research Starters*, EBSCO, www.ebsco.com/research-starters/science/expected-values-mathematical-concept.

Axiom Journal

Mathematical Analysis of the Basic Strategy in Blackjack

Raina Chae

South Korea, Yongsan International School of Seoul

Mathematical Analysis of the Basic Strategy in Blackjack

Raina Chae
South Korea, Yongsan International School of Seoul

Abstract

This paper presents a mathematical analysis of the basic strategy in the game of blackjack, focusing on the optimal decision-making process to maximize expected returns. By modeling the rules of the game, including card values, dealer behavior, and win-loss conditions, we evaluate the outcomes of various player actions such as hitting, standing, doubling down, and splitting. Probabilistic methods are applied to determine the expected values associated with different strategies under standard casino rules. The analysis reveals the effectiveness of the basic strategy compared to random or intuitive play, highlighting the significant impact of informed decision-making on long-term performance.

Keywords: Blackjack, basic strategy, probability, expected value, optimal play, casino mathematics, game theory

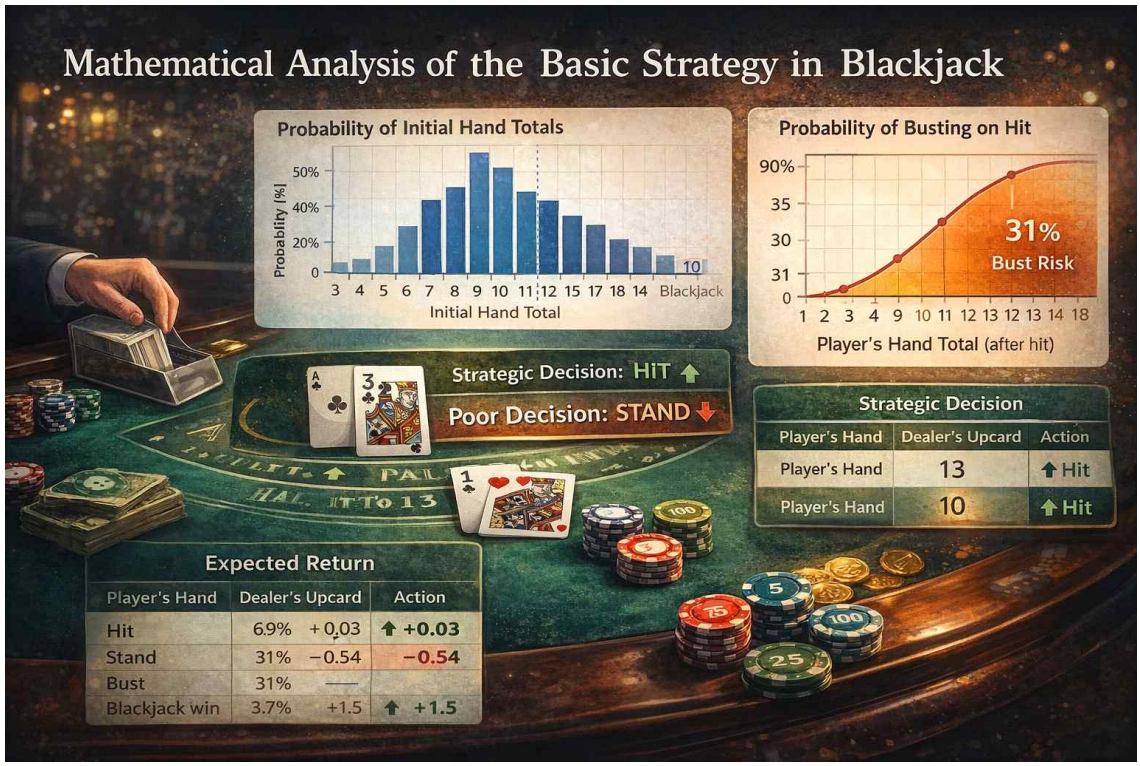

Introduction

Blackjack is a gambling game where a player draws two cards from a deck and plays strategically to beat their opponent. A player has options to choose from after receiving their own card. The most common options are to hit or stand. If a player hits, they may draw another card randomly and add it to their hand. If the value exceeds 21, then the player is bust, meaning that they lose the round, regardless of the opponent's value. If a player stands, they do not draw any cards and keep the total amount until the round is decided.

The goal of blackjack is to be the player with the highest number without exceeding 21. Face cards are worth 10 points, and the Ace can be worth one or eleven points, based on the player's selection of cards. A blackjack signifies an automatic win for the player, as it is seen as an unbeatable card value.

Blackjack Background

Although gambling games, such as blackjack, may be perceived as a game of pure luck, mathematics is combined into the famous game. In mathematics, probability can be used to calculate the chances of an event occurring, helping a player decide on their next move. Also, probability can be used to calculate how likely an event is going to occur. Probability is between the number 0 and 1, when written in decimals, and when it is written as a percentage, it shows the chances of an event occurring. Probability can be modeled in the real world, especially in cases of games. For example, if a player is tossing a coin, the probability formula can be utilized to calculate the chances of receiving either heads or tails. Calculating the probability can be modeled by the equation:

$$\frac{\text{Number of the Best Outcome}}{\text{Total Number of Outcomes}}$$

Therefore, if the player favors heads, the equation can be modeled as $\frac{1}{2}$, as the number of total outcomes is 2 and the best outcome is 1.

In this paper, we will be utilizing probability to model the basic strategy of blackjack, a gambling game that relies on chances and luck. Blackjack is a classic gambling game, where two players go against each other to see who gets a higher number without exceeding the limit of 21. The possible cards are:

- Number Cards (2-10)
- Face Cards (Jack, Queen, King)
- Ace (1 or 11)

Mathematical Analysis of the Strategy

1. Calculation of Receiving a Specific Number

In this section, we will mathematically analyze the calculation of receiving a specific number in blackjack. A standard deck contains 52 cards in total, including:

- 36 Number Cards (2, 3, 4, 5, 6, 7, 8, 9, 10)
- 12 Face Cards (King, Queen, Jack)
- 4 Aces

When playing blackjack, each player receives two cards without any replacement. Therefore, there are 52 choices for the first draw and 51 choices for the second draw. This can be modeled by the equation

$$52 \times 51 = 2652$$

Therefore, there are 2652 possible combinations for a player to draw.

Let us now find the probability of receiving a number from 17 to 20. When a player draws 2 cards from the deck, we look for two card combinations that add up to the number for 17-20. For example, we can find the possible two card combinations for 17:

$$7+10$$
$$10+7$$
$$9+8$$
$$8+9$$
$$A+6$$
$$6+A$$

We would like to know how many total possible combinations there are to draw a 17. Therefore, we can get the total number of the first card and multiply it by the second card.

Table 1 Possible Combinations and Probability of Outcome

Possible Combinations	Multiplication	Probability of Outcome
$7+10$	4×16	64
$10+7$	16×4	64
$9+8$	4×4	16
$8+9$	4×4	16
$A+6$	4×4	16
$6+A$	4×4	16

If we add all the two card combinations, we get

$$64+64+16+16+16+16 = 192$$

There are 192 possible combinations of receiving a combination that adds up to 17.

We can apply the same method for the rest of the cards for 18 - 20.

- The two card combinations for 18 is 172
- The two card combinations for 19 is 160
- The two card combinations for 20 is 272

Adding all these combinations would get us the sum of 1032. Therefore, there are 1032 ways to get a combination that adds up to 17 - 20. We can find the probability of drawing a card from 17 - 20 by dividing 1032 with the total number of outcomes. This can lead to the equation:

$$\frac{N_{17-20}}{N_{total\ outcomes}} = \frac{1032}{2652} \approx 0.3891$$

Therefore, the probability of drawing a card from 17 - 20 is 39%.

Let us now calculate the probability of drawing a card from 11 - 16.

We can use the same method that we used to figure out the total number of combinations for the number 17. Calculating this would lead to:

- 256 combinations of receiving 11
- 230 combinations of receiving 12
- 224 combinations of receiving 13
- 198 combinations of receiving 14
- 192 combinations of receiving 15
- 166 combinations of receiving 16

$$256 + 230 + 224 + 198 + 192 + 166 = 1266$$

This can be applied to the same equation previously used:

$$\frac{N_{11-16}}{N_{total\ outcomes}} = \frac{1266}{2652} \approx 0.4773$$

Thus, the probability of receiving a number from 11 - 16 is 48%.

Finally, let us calculate the probability of receiving a blackjack. The only possible combinations of a blackjack with two cards are an ace and a card worth the value of 10. Since there are 16 cards valued at 10 and 4 aces, the values can be multiplied:

$$A + 10 \rightarrow 4 \times 16 = 64$$

$$10 + A \rightarrow 16 \times 4 = 64$$

Adding these values will get us:

$$64 + 64 = 128$$

Hence, the probability of receiving a blackjack will be

$$\frac{N_{blackjack}}{N_{total\ outcomes}} = \frac{128}{2652} \approx 0.0482$$

The probability of receiving a blackjack from the beginning is 5%.

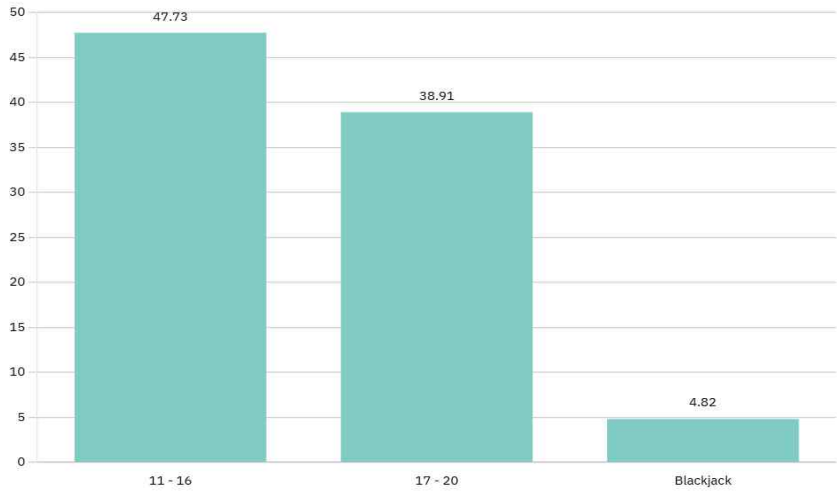

Figure 1 The Probability of Receiving Blackjack

2. Calculation of the Results After Drawing Another Card

Let us look at a case where a player receives a 13 on their draw. In this section, we will calculate the probability of busting, succeeding, or receiving blackjack. We will assume that:

- The deck still has full 52 cards
- The player received a 13
- The player decides to draw another card

Let us define the meaning of the outcomes before the calculation.

- A blackjack will count as the cards adding up to 21
- A success will count the sum of the cards ranging from 14 - 20
- A bust will count as the cards exceeding 21

First, let us calculate the possible outcomes for every card. Organizing the values into a table will get us:

Table 2 Possible Outcomes for Every Card

Draw Value	Total Value	Outcome
2	15	Success
3	16	Success
4	17	Success
5	18	Success
6	19	Success
7	20	Success
8	21	Blackjack
9	22	Bust
10	23	Bust
Jack	23	Bust
Queen	23	Bust
King	23	Bust
Ace (11)	24	Bust
Ace (1)	14	Success

The possible cards that can cause the player to bust are 9, 10, Jack, Queen, King, and potentially Ace. However, since ace can also be counted as a one instead of an eleven, we can remove it from the options. If we number the cards that will cause the player to bust, we can get:

- 4 Cards Valued 9
- 12 Cards Valued 10

Therefore, there are 16 cards that will make the player bust. Since the total number of cards in blackjack is 52, we can divide the 16 cards with the total number of cards in the deck. The same method can be used to calculate the probability of success and the probability of blackjack. There are 28 cards that make the player succeed, and only 4 cards that make the player get blackjack. We can calculate this by doing:

$$Probability\ of\ Bust\ = \frac{16}{52} \approx 31\%$$

$$Probability\ of\ Success = \frac{28}{52} \approx 54\%$$

$$Probability\ of\ Blackjack\ = \frac{4}{52} \approx 8\%$$

Since we took out the Ace card in the probability of bust, the result does not sum up to 100%. However, mentioning the Ace in the probability of bust would make the percentage increase 7%, and this would make the results valid.

In this case, drawing a card is more favorable for the player, as the probability of success is higher compared to the probability of bust and the probability of blackjack. The player has the highest chance to succeed if they draw a random card from the deck.

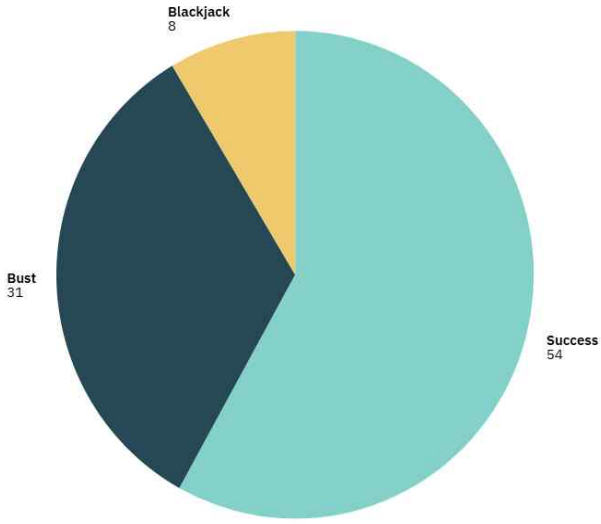

Figure 2 Diagram of Success, Burst, and Blackjack Rate

Conclusion

In this paper, we analyzed the basic professional strategy of black and thoroughly calculated the rate of a player's success after receiving a specific card by applying probability into the game. We also examined the likelihood of the combinations in the initial hand and explored the outcomes of a player after drawing an additional card at the value 13.

The results of the study led to the conclusion that certain numbers, especially ranging from 11 - 16, have a higher chance of occurring in the initial hand. We utilized probability to examine the chances of drawing a number ranging from 17 - 20 and 11 - 16. Then, we utilized the same method to find out the chances of having a blackjack in the start.

Moreover, we analyzed a case in which a player had an initial hand of 13. We considered the mathematical probability of the outcome when a player takes an additional card. The calculations demonstrated that although there is a chance of busting, the probability of success is higher. Therefore, even in real life situations, hitting on an initial hand of 13 would most likely support a player rather than being harmful.

This study highlights that blackjack is not just a game of luck and chance, but a game of calculated analysis, where mathematical probability can be applied to suggest optimal strategies to players. While luck also plays an important role in winning, understanding the probability of winning in a certain situation helps a player make more strategic choices.

Therefore, integrating probability into games of chances and risks can improve a player's decision-making skills and have a better understanding of what they should do for winning games. This is not only applied to blackjack, but mathematical probability can be incorporated with gameplay to improve a player's chances of winning. If a player knows their chances of winning in a situation, it can improve a player's win rate over time.

References

Thorp, Edward O. Beat the Dealer: A Winning Strategy for the Game of Twenty-One. Vintage, 1966.

Griffin, Peter. *The Theory of Blackjack: The Compleat Card Counter's Guide to the Casino, Game of 21.* Huntington Press, 1999.

Epstein, Richard. *The Theory of Gambling and Statistical Logic.* 2nd ed., Academic Press, 2013.

Axiom Journal

Can Mathematical Metrics Detect Bias in AI Decisions?

Matthew Su, Kaian Solomon, Jimmy Thompson, James Cunningham

United States, Millennium High School, 11-12 Grade

Can Mathematical Metrics Detect Bias in AI Decisions?

Matthew Su, Kaian Solomon, Jimmy Thompson, James Cunningham
United States, Millennium High School, 11-12 grade

Abstract

This study assesses the accuracy of mathematical metrics for detecting AI decision-making biases across datasets. With the emerging presence of AI in the modern world, the detection of AI misinformation has become more critical than ever, with AI bias being a central issue. This study analyzes the effectiveness of mathematical metrics for detecting gender bias in AI using a dataset from the UC Irvine repository, employing several methods to test for biases in gender and income data. The mathematical metrics used to detect the AI bias were the Chi-Square test, disparate impact, and statistical parity. The Chi-Square test is the primary method used to detect bias in the AI's decision-making. The analysis found that the AI has a strong bias toward men in the UC Irvine dataset. The AI tended to show a bias towards the gender with the higher count in the dataset, revealing an inherent flaw in using AI to make decisions.

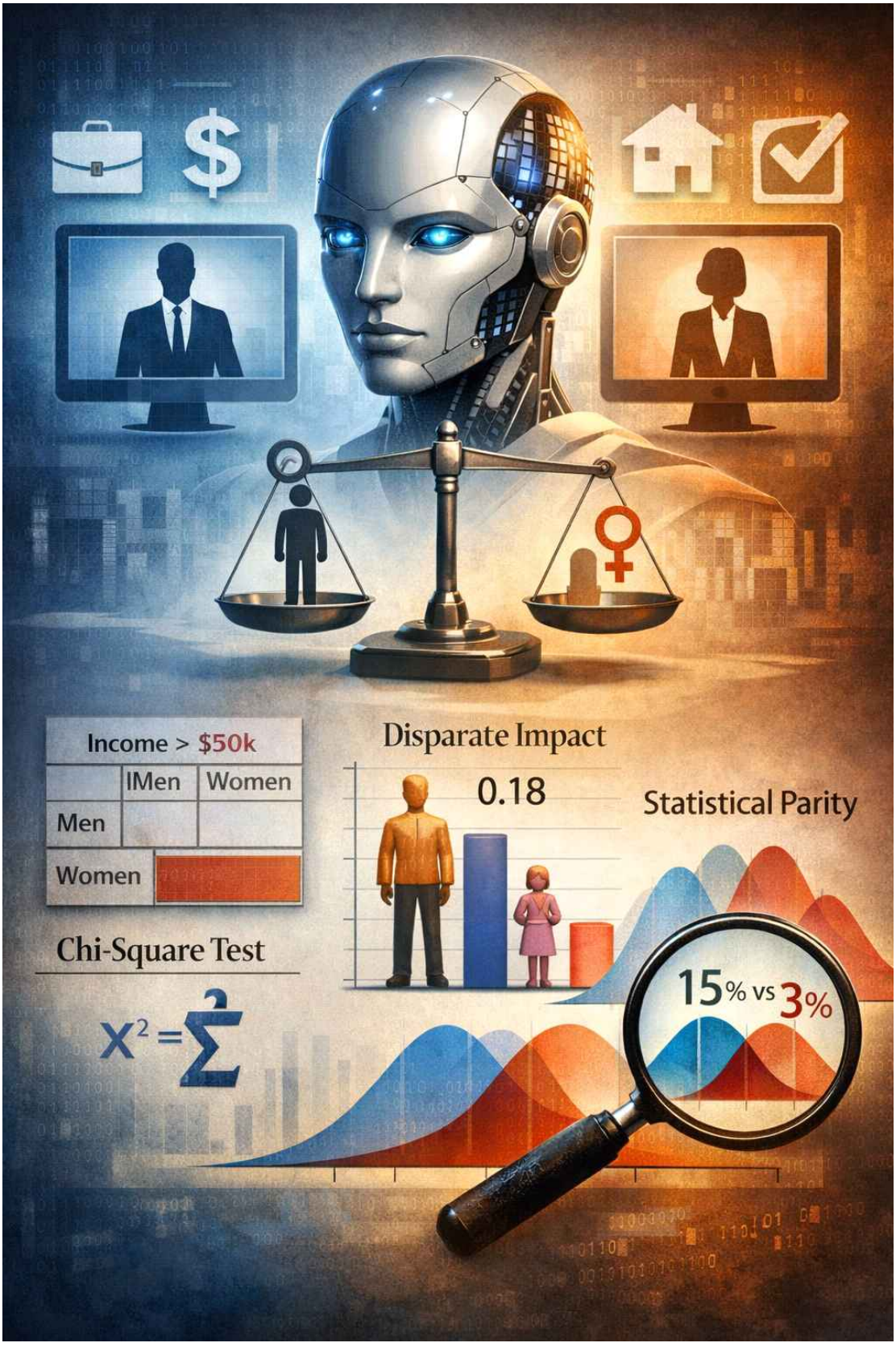
Income > $50k
IMen
Women
Men
Women
Disparate Impact
0.18
Statistical Parity
Chi-Square Test
$X^2 = \sum$
15% vs 3%

Introduction

With Artificial Intelligence embedded in our daily lives, influencing education, decision-making, and media, it is crucial to distinguish between factual information and misinformation. One of the main issues of Artificial Intelligence is that it uses data from the entire internet. Not all sources on the internet are trustworthy, yet AI sometimes uses that information and displays it to the user as factual and correct. This typically happens when AI systems learn from data created by humans, which can lead them to summarize information as an inequality or stereotype based on the data they find. When this biased information is used in real-world applications, such as hiring, loan approvals, or risk assessments, it can result in unfair decisions and controversial outcomes.

Mathematical analysis is a tool that can help detect bias in AI datasets and overall information, allowing us to measure differences between groups using clear, objective numbers. These tools, such as fairness metrics and statistical tests, make it possible to identify whether one group is receiving different outcomes than another, and often whether those differences are larger than chance would predict. Datasets can often be misinterpreted as reflecting stereotypes and inequality if not understood correctly. For example, if a dataset shows that far fewer women earn a given level of high income than men do, a trained AI on that data may mistakenly learn that men are more qualified than women. When patterns like this aren't carefully analyzed, AI systems might take that inequality into account when making decisions, leading to entirely stereotypical choices driven by the dataset's biases.

The overall goal of this project is to use mathematical methods to examine whether gender bias exists in a commonly used income dataset that AI models could potentially be trained on. Ultimately answering the question, "Can Mathematical Methods detect bias within an AI dataset?"

Methods

In this research, we investigate mathematical bias detection in AI decision-making by analyzing whether gender influences income predictions within public datasets. The dataset we used was taken from the UCI Machine Learning Repository's Adult Income Dataset, a source often used to train and test artificial intelligence and run other experiments. This dataset contains real demographics and income information collected in the United States from the 1994 U.S. Census Bureau Database.

In this project, the primary focus was narrowed to two variables within the dataset: gender and income category. The gender variable has only two groups, male and female, while the income variable classifies individuals into two categories: earnings of more than $50,000 per year or $50,000 or less per year. These two variables were chosen because they enable clear, measurable analysis of potential gender-related biases in a dataset often used for AI training. Not only that, these two biases are commonly stereotyped in the real world, which would be great for this experiment.

Information Gathered from the Dataset:

Gender and Earnings	Amount of people
Men Earning > 50k	15,127
Men Earning ≤ 50k	6,662
Women Earning > 50k	1,179
Women Earning ≤ 50k	9,592

Several mathematical metrics were applied to detect bias in AI decision-making. Demographic parity was used to analyze the probability that either men or women would earn more than $50k a year. We defined the protected attribute as each group's gender and identified the positive outcome as earning $50k or more per year. The next step was to determine whether men and women had an equal chance of earning more than $50k per year. This was done by simply calculating the percentage of men who earned more than $50k per year and comparing it to the percentage of women who did. Statistical parity was then used to assess the difference in high-income rates between men and women. This essentially means we subtracted the percentage of men who earned more than $50k per year from the percentage of women who earned more than $50k per year to determine the difference.

The following method utilized was determining the disparate impact ratio. We simply divided the percentage of women who earned $50k or more by the percentage of men who earned $50k or more to get the ratio. The final method to be employed was the Chi-Square Test of

Independence. We first created a contingency table from the dataset. We then calculated the expected counts, determining how many of each gender would make above $50k per year if gender and income were unrelated. The next step was to calculate the four parts of the Chi-Square statistic, then add them to determine whether the difference between gender and income occurs only by chance.

Results

The analysis and methods we used evaluated whether income outcomes differed between men and women using the following metrics: Demographic Parity, Statistical Parity Difference, Disparate Impact, and the Chi-Square Test of Independence (the two-square method). The counts extracted from the Adult Income Dataset from UC Irvine's Machine Learning Repository were used to calculate probabilities, fairness measurements, and the Chi-square Statistic.

DISCLAIMER: Each decimal is rounded to the nearest thousandths

1. Demographic Parity (Probability of Earnings > $50k)

To first determine whether men and women had an equal chance of earning more than $50,000 was to examine the proportion of each gender in the high-income category, which was calculated below:

- Men:

$$P(\text{male} > 50k) = \frac{15127}{15127 + 6662} = 0.694$$

- Women:

$$P(\text{female} > 50k) = \frac{1179}{1179 + 9592} = \text{results}$$

These results suggest that men were significantly more likely than women to earn over $50k.

2. Statistical Parity Difference

This Mathematical Metric measures the difference between the high-income rates of men and women:

$$\text{Statistical Parity Difference} = P(\text{male} > 50k) - P(\text{female} > 50k) = 0.694 - 0.109 = 0.585$$

A difference of 0.585 suggests a significant disparity between the two.

3. Disparate Impact

This Mathematical Metric will help compare the likelihood of women earning > 50k to that of men:

$$\text{Disparate Impact} = \frac{0.109}{0.694} = 0.157$$

A Disparate Impact value below 0.8 indicates potential bias in the Dataset. At 0.157, this result suggests a substantial imbalance.

4. Chi-Square Test of Independence

To determine whether gender and income were statistically related rather than at random, the

chi-square test was applied to the research for further indication. The Chi-square test is a more complex process than the other mathematical metrics, so it is broken down into five steps.

Step 1: Create a contingency table

Gender	>50k	≤50k
Male	15,127	6,662
Female	1,179	9,592

Step 2: Calculate expected counts

Using the table and calculating the totals for each of the genders, along with the income of each of them. Calculate the expected counts: what the numbers would be if gender and income were unrelated.

Expected value: Male > 50k

$$E = \frac{(21{,}789)\ (16{,}306)}{32{,}560} = 10{,}907.899$$

Expected Value: Male ≤ 50k

$$E = \frac{(21{,}789)\ (16{,}254)}{32{,}560} = 10{,}877.100$$

Expected Value: Female > 50k

$$E = \frac{(10{,}771)\ (10{,}306)}{32{,}560} = 5{,}394.100$$

Expected Value: Female ≤ 50k

$$E = \frac{(10{,}771)\ (16{,}254)}{32{,}560} = 5{,}376.\ 899$$

Step 4: Compute each Chi-Square piece

Male > 50k

$$\frac{(15127\ -10907.07)^2}{10907.700} = \frac{4{,}219.3^2}{10{,}881} = 1633.4$$

Male ≤ 50k

$$\frac{(6662\ -\ 10881.3)}{10.881.3} = \frac{4{,}219.3^2}{10{,}907.3} = 1636.8$$

Female > 50k

$$\frac{(1179 - 6398.3)^2}{5398.2} = \frac{4,219.3^2}{5398.3} = 3294.8$$

Female ≤ 50k

$$\frac{(9592 - 5372.7)^2}{5372.7} = \frac{4,219.3^2}{5372.7} = 3312.8$$

Step 5: Add the four values together

$$x^2 = 1633.4 + 1636.8 + 3294.8 + 3312.8$$

$$x^2 = 9,877.8$$

Final Chi-Square Results:

Chi-square= 9877.8

Degrees of Freedom = 1

P-value < 0.00001

There is a strong statistical relationship between gender and income level, indicating that the probability this difference occurred by chance is zero.

Discussion

These results were obtained from mathematical metrics calculated from the Adult Income Dataset, indicating a gender bias, meaning the AI system will conclude that stereotypes exist in these topics. Men were found to have earned above $50k at a much higher rate than women within this dataset. The Statistical Parity Difference shows a 58.5% gap, and the Disparate Impact Ratio of 0.157 is far below the fairness guideline of 0.8, indicating unequal outcomes.

The Chi-square test also confirms a statistically significant association between gender and income. This means the income displayed is highly different and unlikely to be due to random chance. Instead, it is thought to reflect both the real structural inequality captured in the dataset and the inequalities an AI model would learn if trained on this data. In real-world systems such as job screening tools or economic prediction models, this type of imbalance could influence decision-making, ultimately leading to the conclusion that men are more efficient workers than women because they are higher earners. Further research on race could be conducted if desired, but it will likely reach a similar conclusion.

Conclusion

The purpose of this research was simply to detect AI biases in decision-making through mathematical metrics. These mathematical metrics indicate that the difference in the percentage of high-earning individuals between the groups is both very large and unlikely to be due to chance (as noted in the disparate impact ratio and the Chi-Square Test of Independence). Every mathematical metric used showed detectable biases in AI decision-making. This remains important because the use of AI to make decisions is becoming increasingly popular. If we can put mathematical metrics to use and detect biases in AI decision-making, we can prevent users of AI models from misinformation.

References

"Welcome to the UC Irvine Machine Learning Repository." UCI Machine Learning Repository, UC Irvine, archive.ics.uci.edu/. Accessed 9 Nov. 2025.

Axiom Journal

Slowly Decreasing American Band Popularity

Yong Jin Chang

South Korea, Indian Mountain School, 8th Grade

Slowly Decreasing American Band Popularity

Yong Jin Chang
South Korea, Indian Mountain School, 8th Grade

Abstract

This paper compares how quickly people forget different types of music bands. Some bands, like Joy, are one-hit wonders. They become very popular for a short time, but people forget them quickly. Other bands, like New Kids on the Block, have many hit songs and stay popular for a long time. We use a mathematical model to show the remembrance rate over time. The model uses exponential decay to explain how fast the memory of a band fades. We found that Joy's remembrance rate dropped from 100% to 5% in 10 years. But New Kids on the Block kept a higher remembrance rate because they had more songs and loyal fans. This shows how math can be used to understand real-life situations like music popularity.

Keywords: Music popularity, One-hit wonder, Remembrance rate

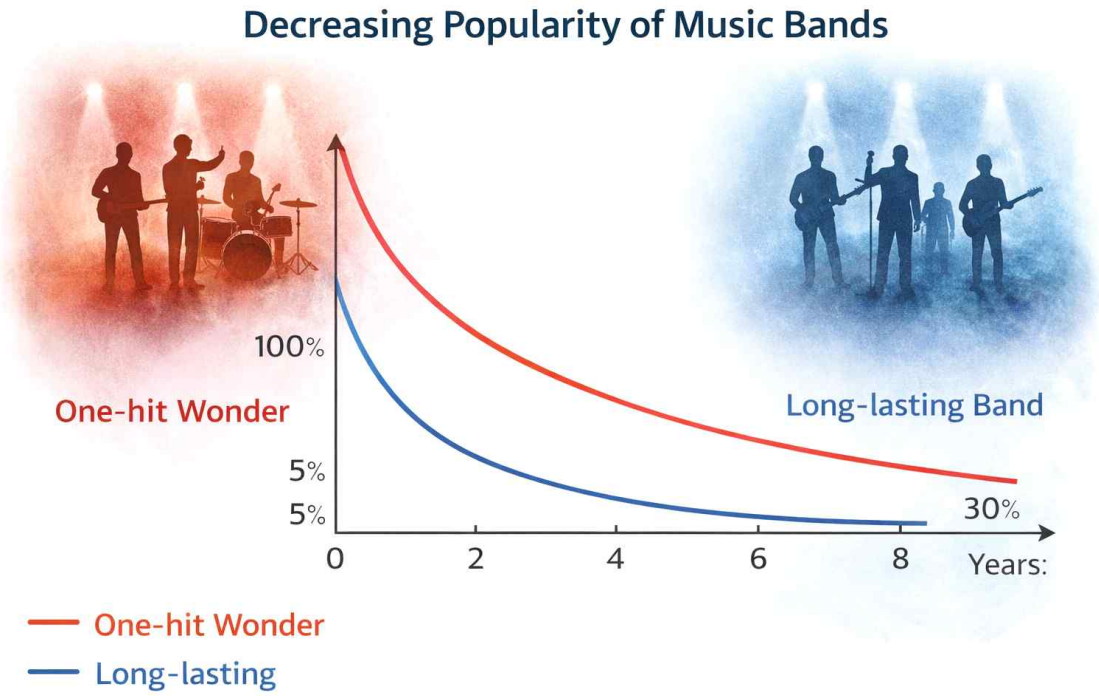

Introduction:

When we imagine a song from the past, some popular bands and songs come to mind right away, while others are harder to remember. We can still picture where we heard a song for a first time, especially the song we loved or the public place we used to hear them for a while.

But over time, even hit songs can start to fade from memory. We wonder: Why do we still remember certain bands so clearly while others seem to disappear in our minds? What helps some artists stay popular for years, while others are forgotten?

One-hit wonder bands and artists often get famous overnight, but then their popularity fades out at the next day. Their song might be heard everywhere for a short time, and everyone seems to know their song. But if the band does not release more hit songs or build a strong fan base, people start to forget them. Their fame fades, and the band becomes just a memory.

However, long-lasting bands keep making songs that people love. They build a loyal group of fans who keep listening, even years later. These bands often stay in our minds longer because their music becomes part of more moments in our lives. We began to wonder if there is a way to show the comparison of one-hit wonder and long-lasting bands' popularity in mathematical approach. We will consider these questions:

- Can we model how fast people forget a band?
- Does having more hit-songs affects to slow down how quickly they are forgotten?

In this paper, we will use a mathematical model to compare how fast people forgot Joy, a one-hit wonder band, with how long they remembered New Kids on the Block, a long-lasting band.

Theoretical Background

Mathematical function that models remembrance rate as it changes with time. In this case, time (t) is measured in years since the band became popular, and the remembrance rate $f(t)$ is the percentage of people who still remember the band at that time. Based on this, we will use this mathematical model:

$$f(t)=\frac{a}{t-p}+q$$

Modeling and Calculation

1. Joy as one-hit wonder band

Figure 1 Joy Band

Studies show that when Joy (Figure 1), as one-hit wonder band, released their hit song, nearly everyone remembered it clearly – 100% remembrance rate at the time of release. However, just a few years later, this memory faded quickly. After about three years, only half of the original audience still remembered the song. After ten years, the remembrance rate dropped to just 5%, meaning almost no one recalled the band or their songs anymore. This rapid decline happened because Joy had only one major hit song. Without more songs or fan interaction, people gradually forgot them. The remembrance rate can be calculated as:

Remembrance rate at the time that an event occurs: 100%

$$f(0)= 100$$

Remembrance rate after 2 years has passed: 50%

$$f(3)= 50$$

Remembrance rate after 10 years has passed: 5%

$$f(10)= 5$$

Therefore:

$$f(0)=-\frac{a}{p}+q=100 \ldots (i)$$

$$f(3)=\frac{a}{3-p}+q=50 \ldots (ii)$$

$$f(10)=\frac{a}{10-p}+q=5 \ldots (iii)$$

2. New Kids on the Block as long-lasting band

Figure 2 New Kids on the Block

In contrast, New Kids on the Block (Figure 2), as a long-lasting band, had a much slower drop in remembrance. Same as Joy, when their music came out, 100% of people remembered their song at first. But even after three years, about 90% of listeners still remembered their songs. After ten years, around 30% of people still recognized their music, which is higher than Joy's remembrance rate, which is 5%. This slower decline of New Kids on the Block's remembrance rate is because they had multiple hit songs and remained an active fan base. Their continued exposure helped keep them in people's memories longer.

Remembrance rate at the time that an event occurs: 100%

$$f(0)=100$$

Remembrance rate after 2 years has passed: 90%

$$f(3)=90$$

Remembrance rate after 10 years has passed: 30%

$$f(10)=30$$

Therefore:

$$f(0)=-\frac{a}{p}+q=100 \ldots (i)$$

$$f(3)=\frac{a}{3-p}+q=90 \ldots (ii)$$

$$f(10)=\frac{a}{10-p}+q=30 \ldots (iii)$$

Conclusion

Music popularity does not last forever, but the speed at which we forget depends on how much the artist stays in our lives. Joy as one-hit wonder band had a hit song but no lasting impact, so people forgot them quickly. On the other hand, New Kids on the Block as long-lasting band stayed popular longer because of their many songs and loyal fans. By using mathematical modeling, we can see this difference. The rational model helps us understand not just what happened to each band, but why it happened. This kind of thinking shows how math can help explain real-life trends — even in something like music.

References

[1] Wikipedia: Joy (Austrian Band)
https://en.wikipedia.org/wiki/Joy_(Austrian_band)
[2] Wikipedia: New Kids on the Block
https://en.wikipedia.org/wiki/New_Kids_on_the_Block

JOURNAL OVERVIEW

About the Journal

Axiom Young Research is an international student research journal that publishes original work in mathematics, science, and interdisciplinary STEM fields.

The journal aims to create a professional environment where young researchers can present their ideas in a formal academic format. By participating in the research and publication process, students gain valuable experience in scientific thinking, problem solving, and scholarly writing.

The journal welcomes submissions in areas including:

- Pure Mathematics
- Applied Mathematics
- Scientific Modeling
- Physics and Natural Sciences
- Computer Science and Artificial Intelligence
- Interdisciplinary STEM Research

All submissions undergo editorial review to ensure clarity, originality, and logical rigor. The journal encourages both individual and collaborative student research projects guided by teachers or mentors.

By making publication opportunities accessible to students around the world, Axiom Young Research seeks to foster a global community of young scholars committed to intellectual exploration.

INTERNATIONAL JOURNAL

AXIOM YOUNG RESEARCH

International Journal of Student Mathematics and Science

VOLUME 2

CONTRIBUTORS

Jinu Yoon

Aisha Shermatova

Hayeon Ku

Raina Chae

Matthew Su, Kaian Solomon, Jimmy Thompson, James Cunningham

Yong Jin Chang

WWW.AXIOMJOURNAL.ORG

EMAIL
admin@axiomjournal.org

ADDRESS
Dept. of Mathematics New Academic Block, University of Delhi, New Delhi 110007 India

MATHEMATICS · APPLIED SCIENCE

SCIENTIFIC MODELING

A PLATFORM FOR THE NEXT GENERATION OF SCIENTISTS

About Axiom Young Research

Axiom Young Research is an international journal dedicated to publishing original scientific and mathematical research conducted by young scholars. The journal provides a professional platform where high school students can present rigorous ideas, develop scientific thinking, and contribute meaningful insights to the global academic community.

The journal welcomes research in areas including:

- Pure Mathematics
- Applied Mathematics
- Scientific Modeling
- Physics and Natural Science
- Computer Science and Artificial Intelligence
- Interdisciplinary STEM research

Each article represents the intellectual curiosity and creativity of the next generation of scientists.

By encouraging rigorous thinking, clear reasoning, and original exploration, Axiom Young Research aims to inspire young researchers to engage deeply with mathematics and science and to share their discoveries with the world.

$ 13.39
53400
9 791193 172506
ISBN 979-11-93172-50-6

www.axiomjournal.org

Published by Axiom Journal